Article

N^1-methylpseudouridylation of mRNA causes +1 ribosomal frameshifting

https://doi.org/10.1038/s41586-023-06800-3

Received: 25 January 2023

Accepted: 31 October 2023

Published online: 06 December 2023

Open access

Check for updates

Thomas E. Mulroney[1], Tuija Pöyry[1], Juan Carlos Yam-Puc[1], Maria Rust[1], Robert F. Harvey[1], Lajos Kalmar[1], Emily Horner[1], Lucy Booth[1], Alexander P. Ferreira[1], Mark Stoneley[1], Ritwick Sawarkar[1], Alexander J. Mentzer[2], Kathryn S. Lilley[3], C. Mark Smales[4,5], Tobias von der Haar[4], Lance Turtle[6], Susanna Dunachie[7,8,9], Paul Klenerman[7,10], James E. D. Thaventhiran[1,11]✉ & Anne E. Willis[1,11]✉

In vitro-transcribed (IVT) mRNAs are modalities that can combat human disease, exemplified by their use as vaccines for severe acute respiratory syndrome coronavirus 2 (SARS-CoV-2). IVT mRNAs are transfected into target cells, where they are translated into recombinant protein, and the biological activity or immunogenicity of the encoded protein exerts an intended therapeutic effect[1,2]. Modified ribonucleotides are commonly incorporated into therapeutic IVT mRNAs to decrease their innate immunogenicity[3–5], but their effects on mRNA translation fidelity have not been fully explored. Here we demonstrate that incorporation of N^1-methylpseudouridine into mRNA results in +1 ribosomal frameshifting in vitro and that cellular immunity in mice and humans to +1 frameshifted products from BNT162b2 vaccine mRNA translation occurs after vaccination. The +1 ribosome frameshifting observed is probably a consequence of N^1-methylpseudouridine-induced ribosome stalling during IVT mRNA translation, with frameshifting occurring at ribosome slippery sequences. However, we demonstrate that synonymous targeting of such slippery sequences provides an effective strategy to reduce the production of frameshifted products. Overall, these data increase our understanding of how modified ribonucleotides affect the fidelity of mRNA translation, and although there are no adverse outcomes reported from mistranslation of mRNA-based SARS-CoV-2 vaccines in humans, these data highlight potential off-target effects for future mRNA-based therapeutics and demonstrate the requirement for sequence optimization.

A key feature of therapeutic IVT mRNAs is that they contain modified ribonucleotides, which have been shown to decrease innate immunogenicity and can additionally increase mRNA stability, both of which are favourable characteristics for mRNA therapies[1–5]. For example, clinically approved SARS-CoV-2 mRNA vaccines incorporate N^1-methylpseudouridine (1-methylΨ), which has been shown to decrease IVT mRNA innate immunogenicity[3–5]. Some modified ribonucleotides, such as 5-methylcytidine (5-methylC), are naturally occurring post-transcriptional mRNA modifications in eukaryotes, whereas others are not, such as 1-methylΨ (refs. 6–10).

We investigated how 5-methoxyuridine (5-methoxyU), 5-methylC and 1-methylΨ affect translation of IVT mRNA. 5-methoxyU, 5-methylC and 1-methylΨ have been utilized in IVT mRNAs to attempt to increase recombinant protein synthesis in vitro, and for preclinical proof of concept for IVT mRNA-based therapies[11,12]. As mentioned, 1-methylΨ is a ribonucleotide incorporated in licensed IVT mRNA-based SARS-CoV-2 vaccines, but also mRNA-based human vaccines and therapies in development[2,13,14].

Despite their widespread use, surprisingly little is known about how ribonucleotide modification affects protein synthesis, particularly for translation of therapeutic IVT mRNAs. We were interested in how modified ribonucleotides affect the fidelity of mRNA translation for several reasons. Certain ribonucleotide modifications can recode mRNA sequences (for example, inosine[15]). 5-methylC has previously been shown to increase misreading during mRNA translation in prokaryotes, but its effect on eukaryotic mRNA translation fidelity has not been explored[16]. The effect of 5-methoxyU on translation fidelity has not been investigated. Pseudouridine (Ψ) is known to increase misreading of mRNA stop codons in eukaryotes, and can affect misreading during prokaryotic mRNA translation[16–18]. 1-methylΨ does not seem to affect codon misreading, but has been shown to affect protein synthesis rates and ribosome density on mRNAs, suggesting a direct effect on mRNA translation[19,20].

[1]MRC Toxicology Unit, University of Cambridge, Cambridge, UK. [2]Wellcome Centre for Human Genetics, University of Oxford, Oxford, UK. [3]Department of Biochemistry, University of Cambridge, Cambridge, UK. [4]School of Biosciences, Division of Natural Sciences, University of Kent, Canterbury, UK. [5]National Institute for Bioprocessing Research and Training, University College Dublin, Foster Avenue, Mount Merrion, Dublin, Ireland. [6]NIHR Health Protection Research Unit for Emerging and Zoonotic Infections, Institute of Infection, Veterinary and Ecological Sciences, University of Liverpool, Liverpool, UK. [7]NIHR Oxford Biomedical Research Centre, Oxford University Hospitals NHS Foundation Trust, Oxford, UK. [8]NDM Centre for Global Health Research, Nuffield Department of Medicine, University of Oxford, Oxford, UK. [9]Mahidol-Oxford Tropical Medicine Research Unit, Mahidol University, Bangkok, Thailand. [10]Translational Gastroenterology Unit, Nuffield Department of Medicine, University of Oxford, Oxford, UK. [11]These authors contributed equally: James E. D. Thaventhiran, Anne E. Willis. ✉e-mail: jedt2@cam.ac.uk; aew80@cam.ac.uk

At present, it is unclear which modified ribonucleotides affect mRNA translation fidelity and existing studies are mostly limited to understanding misreading frequencies only at a given codon. Misreading of mRNA codons is also only one type of post-transcriptional mechanism that can alter a polypeptide sequence. So far, no study has investigated the fundamental question of whether modified ribonucleotides can affect the maintenance of the correct reading frame during translation of a synthetic transcript. Understanding these processes is critical to increase our knowledge of protein synthesis from modified mRNAs in general, but is also imperative for the robust design and evaluation of new mRNA-based therapeutics that make use of modified ribonucleotides within widely differing RNA sequences or therapeutic contexts.

To investigate how ribonucleotide modification affects reading frame maintenance during translation of mRNA, we designed and synthesized IVT mRNAs (Fluc+1FS) that report on out-of-frame protein synthesis (Fig. 1a). Fluc+1FS mRNAs encode an amino-terminal segment of firefly luciferase (NFluc) and a complementary carboxy-terminal segment of Fluc (CFluc), directly downstream. CFluc is encoded in the +1 reading frame. Fluc+1FS mRNAs are designed to produce catalytically inactive (truncated) NFluc when translated normally. However, if ribosomes move out of frame during translation, elongated polypeptides containing residues from both in-frame NFluc and out-of-frame CFluc can be produced, which can increase catalytic activity.

We synthesized unmodified Fluc+1FS mRNAs, which contain canonical ribonucleotides, and translated them in vitro. We confirmed that Fluc+1FS mRNAs produce catalytically inactive NFluc (Extended Data Fig. 1). By comparison, unmodified wild-type (WT) Fluc mRNA, containing the complete in-frame Fluc coding sequence, produced the expected active protein (Extended Data Fig. 1). Then we synthesized and translated each mRNA containing 5-methoxyU, 5-methylC, 1-methylΨ, 5-methoxyU + 5-methylC or 1-methylΨ + 5-methylC. Translation of WT Fluc mRNA was not significantly affected by either 1-methylΨ or 5-methylC modifications alone, but was decreased by incorporating both ribonucleotides into a single transcript (Fig. 1b). 5-methoxyU incorporation alone, or combined with 5-methylC, significantly decreased translation of WT Fluc mRNA (Fig. 1b). Incorporation of 1-methylΨ in Fluc+1FS mRNA significantly increased ribosomal +1 frameshifting to about 8% of the corresponding in-frame protein, which was not observed for other ribonucleotides (Fig. 1c). HeLa cells transfected with 1-methylΨ Fluc+1FS mRNA recapitulated the results from in vitro translation (Fig. 1d). On the basis of these observations, we concluded that IVT mRNA containing 1-methylΨ or 5-methylC exhibits similar translation efficiency to unmodified mRNA, but 1-methylΨ significantly increases ribosomal +1 frameshifting during mRNA translation.

We observed a large increase in ribosomal +1 frameshifting during translation of 1-methylΨ mRNA and reasoned that gaining better understanding of the translation products would complement the reporter assay data and help to explain how +1 frameshifted products originate. To address these aspects, we probed the polypeptides produced during IVT mRNA translation by western blotting. Translation of unmodified Fluc+1FS mRNA produced the expected in-frame truncated product, which was also true for 5-methylC mRNA (Fig. 1e). Translation of 1-methylΨ mRNA produced the expected in-frame product, but also produced two additional bands at higher molecular weight (Fig. 1e). We reasoned that these products were +1 frameshifted polypeptides. We also confirmed that 1-methylΨ + 5-methylC-, 5-methoxyU- and 5-methoxyU + 5-methylC mRNAs were comparatively poor mRNA templates for protein synthesis (Fig. 1e).

1-methylΨ is also used in clinically approved SARS-CoV-2 mRNA vaccines[3,4]. As 1-methylΨ increased +1 ribosome frameshifting during translation in vitro, we investigated whether this occurs in vivo for BNT162b2, a SARS-CoV-2 mRNA vaccine containing 1-methylΨ. We reasoned that +1 ribosomal frameshifting during recombinant antigen mRNA translation could lead to presentation of +1 frameshifted products to T cells, and elicit off-target cellular immune responses

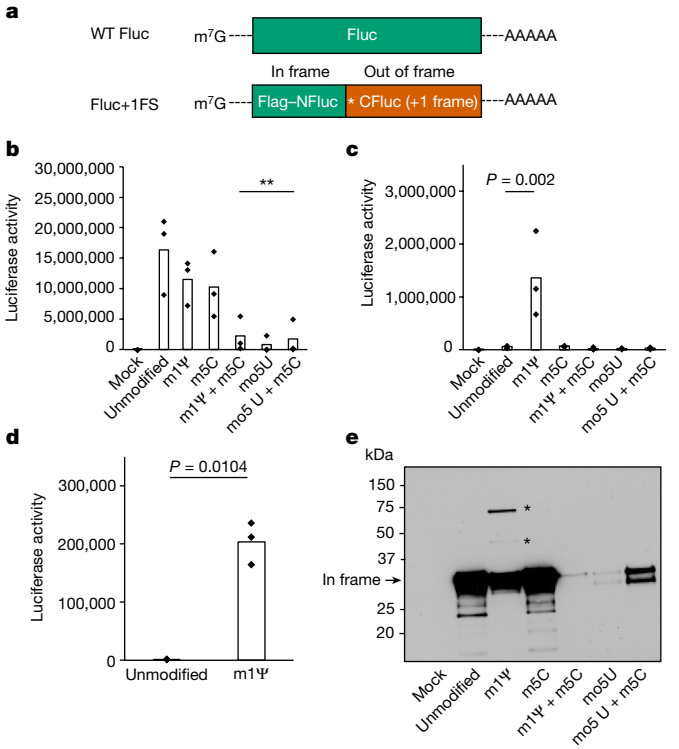

Fig. 1 | Translation of 1-methylΨ-modified mRNA produces +1 frameshifted polypeptides. a, Structures of IVT mRNA transcripts used to probe protein synthesis fidelity. WT Fluc contains only (in-frame) Fluc coding sequence. For Fluc+1FS, the green segment represents in-frame N-terminal Fluc coding sequence (NFluc), and the orange segment represents +1 frameshifted C-terminal Fluc coding sequence (CFluc). Asterisk represents a premature stop codon. **b**, Luciferase activity produced by translation of WT Fluc mRNAs, either unmodified control (canonical nucleotides), or containing 1-methylΨ (m1Ψ), 5-methylC (m5C), 5-methoxyU (mo5U) or the combinations indicated. $^{**}P < 0.01$ (1-methylΨ + 5-methylC, $P = 0.0051$; 5-methoxyU, $P = 0.0023$; 5-methoxyU + 5-methylC, $P = 0.0042$; one-way analysis of variance (ANOVA) with Dunnett's test). **c**, Luciferase activity produced by translation of modified Fluc+1FS mRNAs and unmodified control. 1-methylΨ, $P = 0.002$ (one-way ANOVA with Dunnett's test). **d**, Luciferase activity in lysates produced by transfection of HeLa cells with unmodified or 1-methylΨ Fluc+1FS mRNA for 8 h. $P = 0.0104$ (Welch's one-tailed t-test). **e**, Western blot analysis (anti-Flag epitope) of polypeptides produced by translation of mRNAs in **c**. All data are obtained from $n = 3$ replicated experiments. **e** shows a single blot from $n = 3$ replicated experiments. Asterisks represent bands at higher molecular weight. For gel source data, see Supplementary Fig. 2.

(Fig. 2a). Antigen presentation from mistranslation of endogenous tumour mRNA has been shown to occur in vivo (for example, ref. 21). To address this possibility, we vaccinated mice with BNT162b2 and quantified their T cell response to in-frame SARS-CoV-2 spike protein and +1 frameshifted products predicted to occur by translation of the mRNA +1 frame, as well as an unrelated control antigen (SARS-CoV-2 M protein), by interferon-γ (IFNγ) ELISpot assay. Junction peptides consisting of in-frame N-terminal residues and C-terminal +1 frameshifted residues were not included. We found that responses to +1 frameshifted spike peptides were significantly increased in vaccinated mice compared to untreated mice or those vaccinated with ChAdOx nCoV-19, which does not produce antigen from translation of N^1-methylpseudouridylated mRNA[22] (Fig. 2b). Both BNT162b2 and ChAdOx1 nCoV-19 vaccination produced ELISpot responses to in-frame SARS-CoV-2 spike (Fig. 2c). These data suggest that +1 frameshifted products encoded in BNT162b2 spike mRNA are T cell antigens for inbred mice, to which off-target immunity can be detected following vaccination.

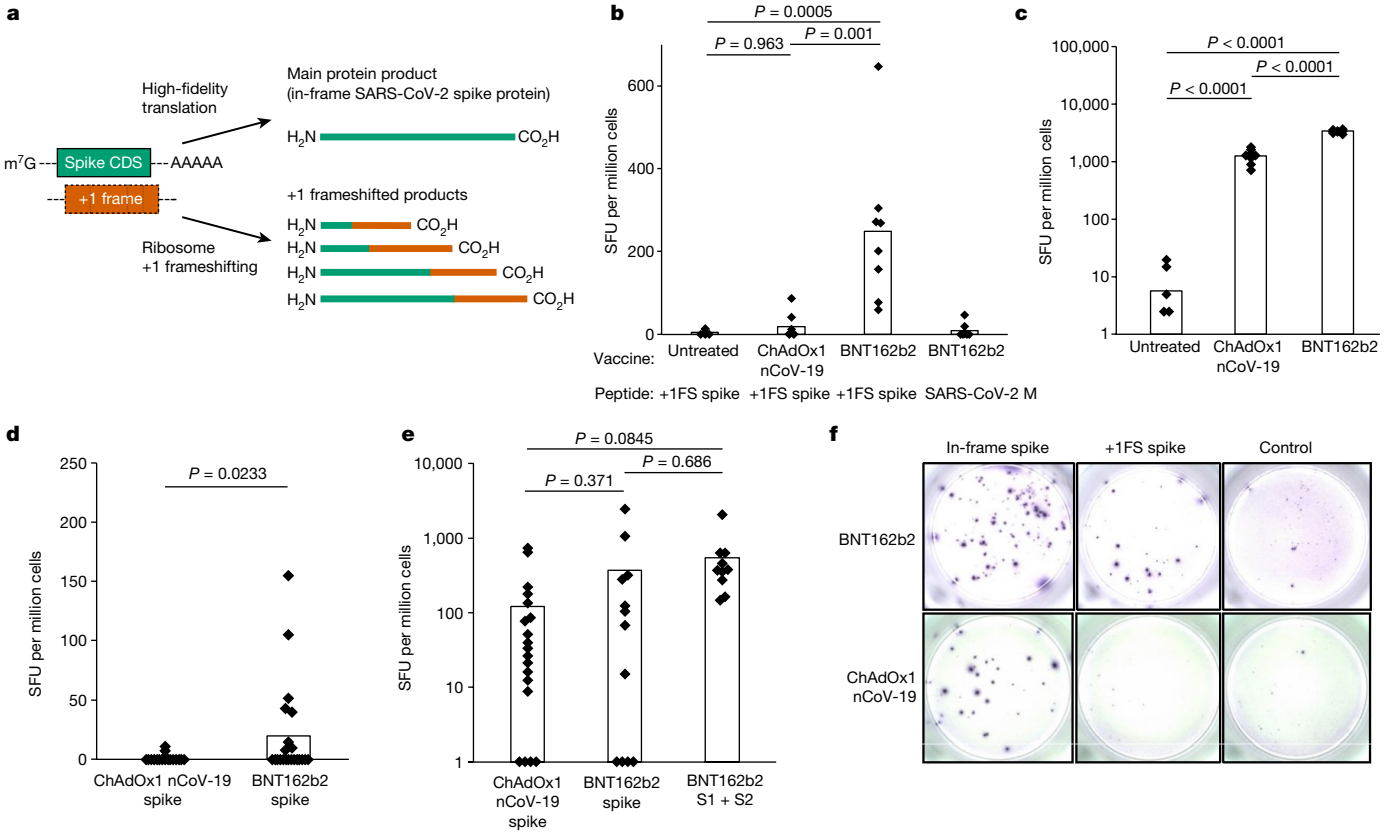

Fig. 2 | +1 frameshifted products elicit off-target cellular immune responses following modified mRNA vaccination. a, Depiction of spike and +1 frameshifted (+1FS) products produced by 1-methylΨ-modified spike mRNA translation. CDS, coding sequence. **b**, Splenocyte IFNγ ELISpot responses from untreated, ChAdOx1 nCoV-19-vaccinated or BNT162b2-vaccinated mice stimulated with +1FS spike peptides. IFNγ ELISpot response from BNT162b2-vaccinated mice stimulated with SARS-CoV-2 M peptides (unrelated control antigen) is included for additional comparison. SFU, spot-forming units. Each group $n = 8$. Untreated versus ChAdOx1 nCoV-19, $P = 0.963$; untreated versus BNT162b2, $P = 0.0005$; ChAdOx1 nCoV-19 versus BNT162b2, $P = 0.001$. **c**, Splenocyte IFNγ ELISpot responses from mice in **b** stimulated with spike peptides. Untreated versus ChAdOx1 nCoV-19, $P = 2.05 \times 10^{-9}$; untreated versus BNT162b2, $P = 4.5 \times 10^{-14}$; ChAdOx1 nCoV-19 versus BNT162b2, $P = 1.88 \times 10^{-13}$. **d**, Peripheral blood mononuclear cells (PBMC) IFNγ ELISpot responses from donors vaccinated with ChAdOx1 nCoV-19 ($n = 20$) or BNT162b2 ($n = 21$) stimulated with +1FS spike peptides. $P = 0.0233$ (Welch's one-tailed t-test). **e**, PBMC IFNγ ELISpot responses from donors in **c** stimulated with in-frame spike peptides: total spike pool or spike S1 + S2 subpools. ChAdOx1 nCoV-19 spike versus BNT162b2 spike, $P = 0.371$; ChAdOx1 nCoV-19 spike versus BNT162b2 S1 + S2, $P = 0.0845$; BNT162b2 spike versus BNT162b2 S1 + S2, $P = 0.686$. **f**, Representative images of PBMC IFNγ ELISpot response wells for two individuals vaccinated with either BNT162b2 responder (top) or ChAdOx1 nCoV-19 (bottom). Left to right: in-frame spike response (spike peptides); +1FS spike response (+1FS spike peptides); no peptide control. P values in **b**,**c**,**e** were determined by one-way ANOVA and Tukey's test.

We then compared IFNγ ELISpot responses to predicted +1 frameshifted SARS-CoV-2 spike protein products in 21 individuals vaccinated with BNT162b2 and compared these responses to those of 20 individuals vaccinated with ChAdOx1 nCoV-19, none of whom reported undue effects as a result of vaccination. We detected a significantly higher IFNγ response to +1 frameshifted antigen in the BNT162b2 vaccine group, compared to ChAdOx1 nCoV-19 (Fig. 2d). There was no association between T cell responses to +1 frameshifted antigen and age, sex or HLA subtype (Supplementary Table 1 and Extended Data Figs. 2 and 3). Both ChAdOx1 nCoV-19 and BNT162b2 vaccination produced ELISpot responses to in-frame SARS-CoV-2 spike, but responses to +1 frameshifted products were observed only in individuals vaccinated with BNT162b2 (Fig. 2e,f). During SARS-CoV-2 viral replication, a programmed −1 ribosomal frameshift occurs naturally during translation of open reading frame (ORF) 1a and ORF1b (ref. 23). It is not feasible that these data are a consequence of natural SARS-CoV-2 infection for the following, non-exhaustive, reasons. First, no frameshifting activity is known to occur during SARS-CoV-2 spike subgenomic mRNA translation (which would be a major discovery in its own right). Second, −1 frameshifting (and not +1 frameshifting) is restricted to a single programmed site in ORF1a and ORF1b (ref. 23). Third, +1 frameshifted peptides are predicted from the BNT162b2 mRNA sequence, and not the S gene sequence from wild virus (Extended Data Fig. 4). Instead, these data suggest that vaccination with 1-methylΨ mRNA can elicit cellular immunity to peptide antigens produced by +1 ribosomal frameshifting in both major histocompatibility complex (MHC)-diverse people and MHC-uniform mice.

To provide further mechanistic insight into +1 ribosome frameshifting during translation of 1-methylΨ mRNA, and identify potential frameshift sites or sequences, we translated 1-methylΨ Fluc+1FS mRNA, purified the major putative +1 frameshifted polypeptide and carried out liquid chromatography tandem mass spectrometry (LC–MS/MS) of tryptic digests. From this single polypeptide, we identified six in-frame peptides and nine peptides derived from the mRNA +1 frame (Fig. 3a and Extended Data Table 1). All in-frame peptides were mapped to the N-terminal region, whereas +1 frameshifted peptides were mapped downstream (Fig. 3a). We then repeated this analysis using a different protease and identified a junction peptide spanning the main frame and the +1 frame (Fig. 3b). These data demonstrated that the elongated polypeptide was indeed a chimeric polypeptide consisting of in-frame N-terminal residues and +1 frameshifted C-terminal residues. As expected, shorter frameshifted products

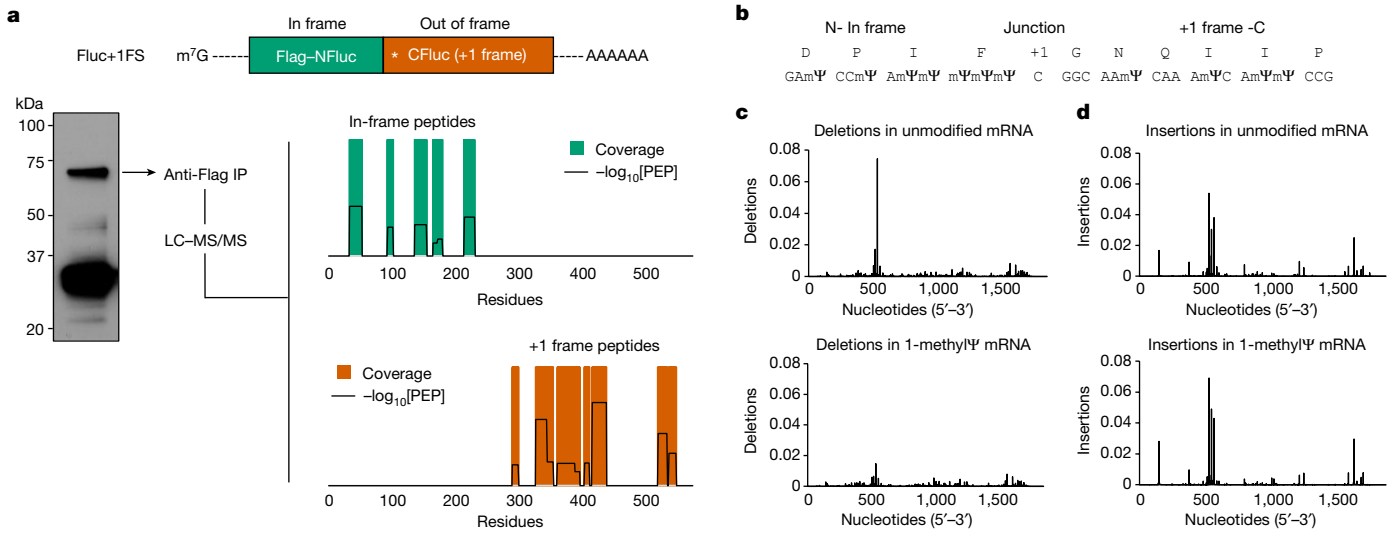

Fig. 3 | Mistranslation of 1-methylΨ mRNA is due to +1 ribosomal frameshifting and not transcriptional errors. a, Tryptic peptide coverage plot of the purified high molecular weight polypeptide produced by translation of 1-methylΨ Fluc+1FS mRNA, showing in-frame residues (top) and +1 frameshifted residues (bottom). $-\log_{10}$[PEP] is the mass spectrum percolator score (only high-quality peptides are shown). IP, immunoprecipitate. The structure of Fluc+1FS mRNA from Fig. 1 is re-displayed and a western blot of the translation reaction before immunoprecipitation is displayed. For gel source data, see Supplementary Fig. 3. **b**, Junction peptide derived from +1 ribosomal frameshifting and the originating mRNA sequence. **c**, Nucleotide deletions in unmodified (top) and 1-methylΨ (bottom) Fluc+1FS mRNA, quantified by $n = 3$ RNA-sequencing analyses. **d**, Nucleotide insertions in unmodified (top) and 1-methylΨ (bottom) Fluc+1FS mRNA.

were also produced from translation of 1-methylΨ mRNA encoding full-length Fluc (Extended Data Fig. 5).

Apparent errors in protein synthesis, including frameshifting, can be consequences of DNA mutation or transcriptional errors[24]. Hence, faithful translation of an incorrect mRNA sequence can produce incorrect proteins. In vitro transcripts are presumed to be exact RNA copies of template DNA, the accuracy of which may be estimated by the fidelity of the used RNA polymerase. However, the substitution of canonical substrate ribonucleoside triphosphates for modified nucleotides may increase transcriptional errors. To address this possibility, we carried out high-throughput RNA sequencing of unmodified and 1-methylΨ Fluc+1FS mRNA and quantified nucleotide insertions and deletions in each population of IVT mRNA. Nucleotide deletion profiles for each mRNA were very similar (Fig. 3c), as were nucleotide insertions (Fig. 3d), suggesting few site-specific differences. The overall frequency of insertions and deletions was low, and did not differ significantly between unmodified and 1-methylΨ mRNA (Extended Data Table 2), which is supported by recent observations[25]. From these findings, we concluded that frameshifted products of 1-methylΨ mRNA translation were not due to transcriptional errors, but were due to bona fide ribosomal +1 frameshifting—a post-transcriptional mechanism.

Ribosome frameshifting is a well-documented phenomenon that occurs during translation of many naturally occurring mRNAs[24]. As ribosome stalling is implicated in several instances of +1 frameshifting, we queried how the presence of 1-methylΨ in IVT mRNA affects translation elongation[26–28]. To do this, we assayed protein synthesis during translation of unmodified or 1-methylΨ WT Fluc mRNA using co-translational [^{35}S]methionine labelling[29]. Translation elongation of 1-methylΨ mRNA was slower than for unmodified mRNA (Fig. 4a), which is supported by previous observations[20]. All reactions were run for 30 min and there was less full-length protein produced from the translation of 1-methylΨ-containing mRNAs, suggesting a slower elongation rate compared to that of unmodified mRNA, with a greater proportion of premature polypeptide products. These data suggested that elongating ribosomes stall during translation of mRNA containing 1-methylΨ.

It was unclear whether 1-methylΨ affected mRNA decoding rates, or another process, during elongation. We reasoned that slower decoding of 1-methylΨ codons during translation elongation could lead to ribosome stalling, similar to previous observations for 'hungry' codons at sites of +1 frameshifting during translation of naturally occurring mRNA[21,28]. We probed the molecular mechanism of ribosome stalling during 1-methylΨ mRNA translation using the aminoglycoside paromomycin. In brief, during mRNA decoding, cognate aminoacyl-tRNA anticodon–codon interaction causes local conformational changes in 18S rRNA (in eukaryotes), after which a new peptide bond is formed, ribosome subunit rotation occurs, and subsequent ribosome conformational changes, elongation factor 2 binding and translocation to the next codon completes the elongation cycle[30]. Paromomycin binds to helix 44 of 18S rRNA in elongating ribosomes and alters its conformation in the decoding centre, which inhibits translation but also permits the productive binding of near- and non-cognate aminoacyl-tRNAs to the 80S ribosome A-site[31]. In doing so, paromomycin increases the misincorporation of amino acids into elongating polypeptides[32]. We reasoned that if slow decoding during 1-methylΨ mRNA translation was due to altered aminoacyl-tRNA binding kinetics, this process could be decreased by paromomycin. This is because paromomycin-bound ribosomes could incorporate additional near- or non-cognate aminoacyl-tRNAs and effectively increase the substrate aminoacyl-tRNA pool at ribosome stall sites. Translation of 1-methylΨ mRNA was slower than that of unmodified mRNA and the proportion of premature polypeptide products was greater (Fig. 4a). However, during 1-methylΨ mRNA translation, polypeptide elongation was improved by the addition of paromomycin, whereas paromomycin was inhibitory only to unmodified mRNA translation (Fig. 4a). Together, these data show that slow translation of 1-methylΨ mRNA is probably due to ribosome stalling, which is caused by altered aminoacyl-tRNA binding, and which can be rescued by increasing the incorporation of near- or non-cognate amino acids into elongating polypeptides.

Although there is no evidence that frameshifted products in humans generated from BNT162b2 vaccination are associated with adverse outcomes, for future use of mRNA technology it is important that mRNA sequence design is modified to reduce ribosome frameshifting

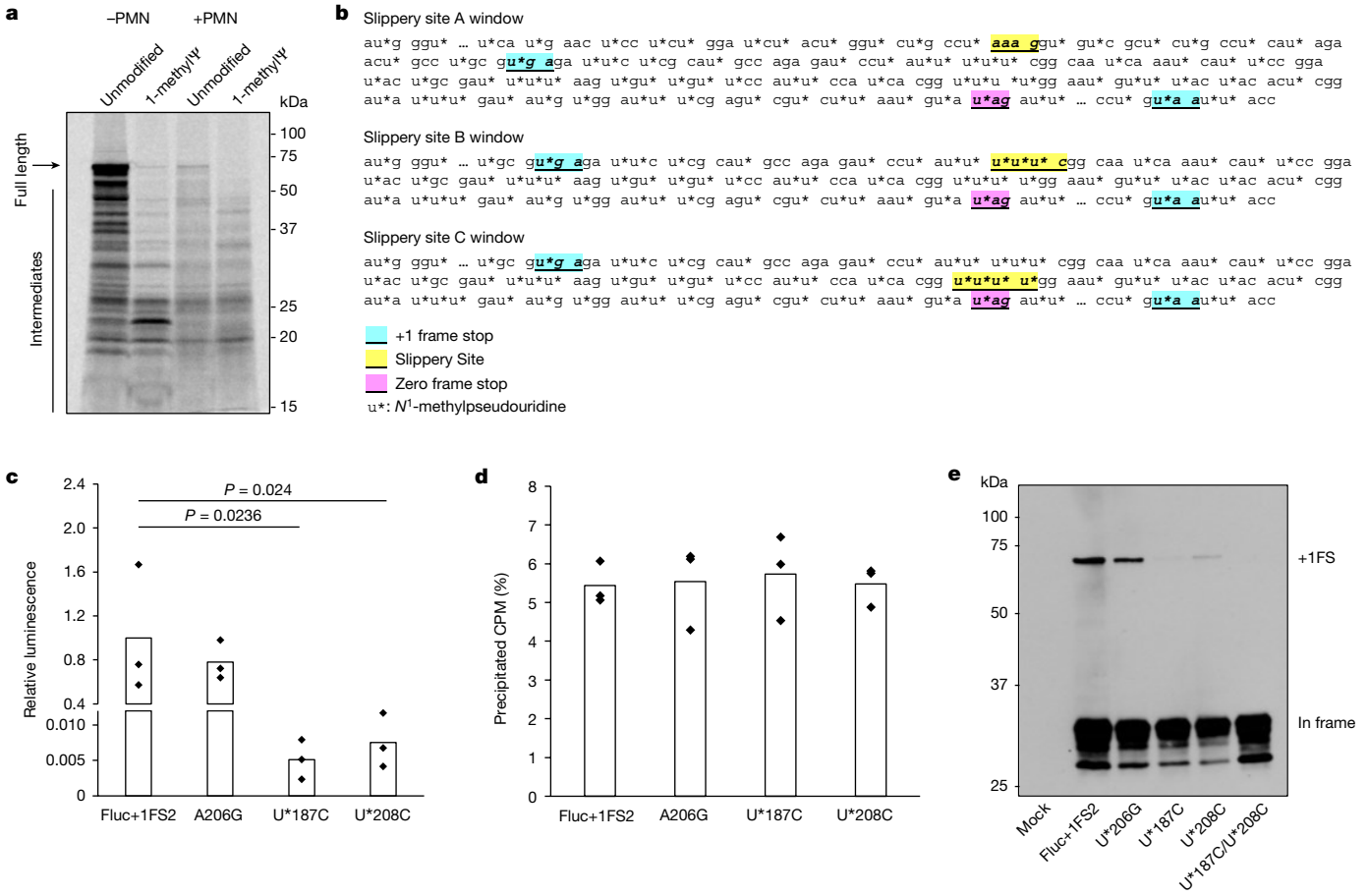

Fig. 4 | +1 ribosomal frameshifting is dependent on mRNA slippery sequences and associated with ribosome stalling during 1-methylΨ mRNA translation. a, SDS–polyacrylamide gel electrophoresis autoradiograph of [^{35}S] methionine-labelled polypeptides produced by translation of unmodified or 1-methylΨ Fluc mRNA for 30 min, including or omitting 100 μM paromomycin (+PMN and –PMN, respectively). **b**, Diagram showing putative mRNA slippery sequences and stop-codon-flanked windows. **c**, Activity of +1 frameshifted products after translation of 1-methylΨ mutant mRNAs, or 1-methylΨ Fluc+1FS2 control mRNA, for 2 h. Fluc+1FS2 versus U*187C, $P = 0.024$; Fluc+1FS2 versus U*208C, $P = 0.0236$ (one-way ANOVA with Dunnett's test). **d**, Total mRNA translation over 2 h for each of Fluc+1FS2 mRNA or mutant mRNAs, quantified by [^{35}S]methionine incorporation. CPM, counts per minute. **e**, Western blot analysis (anti-Flag epitope) of polypeptides produced by translation of mRNAs in **c**, and U*187C/U*208C double-mutant 1-methylΨ mRNA. Data are from $n = 3$ replicated experiments. **a** and **e** show representative images from $n = 3$ replicated experiments. For gel source data, see Supplementary Figs. 4 and 5.

events, as this may limit its future use for applications that require higher doses or more frequent dosing, such as the in vivo production of hormones. It is important to continue investigating therapeutic mRNA mistranslation and immunogenicity, as the evolution of antibody and cytolytic T cell responses against +1 frameshifted spike variants and peptides has not been systematically evaluated in humans and ELISpot responses obtained from pooled peptides may also underestimate T cell responses. The main in-frame mRNA-encoded product is unlikely to elicit an adaptive immune response, but presentation of +1 frameshifted products could activate T cells that target host cells. We reasoned that if we were able to identify +1 ribosome frameshift sites or sequences it would be possible to alter the mRNA sequence to reduce such effects. As proof of principle, we used our reporter IVT mRNA system. LC–MS/MS analysis showed that translation of 1-methylΨ mRNA leads to synthesis of +1 frameshifted products within the area of coding sequence between detected in-frame residues and downstream +1 frameshifted residues (Fig. 3a). We searched the RNA sequence corresponding to this region in the junction peptide coding sequence (Fig. 3b) and determinants of ribosome frameshifting from published mechanisms, from which we identified three potential ribosome slippery sequences (Fig. 4c), with all three sequences having the potential to be decoded by the same aminoacyl-tRNA at an in-frame codon or in the immediate +1 frame codon. Notably, six slippery sites identical to Fluc+1FS slippery sites B and C were also distributed in the BNT162b2 spike mRNA coding sequence. These sites have been annotated in the Fluc+1FS coding sequence (Fig. 4b) and the BNT163b2 spike mRNA coding sequence (Extended Data Fig. 6). We reasoned that these sequences could therefore function as sites for +1 ribosomal frameshifting. We synonymously mutated each site in 1-methylΨ Fluc+1FS mRNA such that the in-frame amino acid was unchanged, but the immediate +1 frame codon was mutated to a non-cognate amino acid, hence destroying the ribosome slippery sequence, and translated the mRNAs to evaluate the contribution of each site to +1 ribosomal frameshifting (Fig. 4c). A +1 frame stop codon was present downstream of slippery site A, and it was unlikely that frameshifting at this site contributed to increased luciferase activity. As expected, luciferase activity produced by translation of site A mutant A206G mRNA was the same as control levels (Fig. 4c). However, both slippery site B mutant U*187C mRNA and slippery site C mutant U*208C mRNA strongly decreased +1 ribosome frameshifting (Fig. 4c). Notably, translation efficiency of each mRNA was equal, which suggests that no mutation adversely affected mRNA translation overall, but solely +1 ribosomal frameshifting activity (Fig. 4d). Translation of a U*187C/U*208C double-mutant 1-methylΨ Fluc+1FS mRNA produced no detectable +1 ribosome frameshifting (Fig. 4e). The transframe protein product predicted by +1 frameshifting at slippery site C contains an alteration of 19 amino acid residues

(compared to WT Fluc), whereas +1 frameshifting at slippery site B produces a transframe product that is effectively 100% homologous to WT Fluc. In addition, given that mutation of either slippery site B or C (U*187C or U*208C) significantly decreased luciferase activity, but that relatively more frameshifted product was produced by translation of U*208C mRNA (Fig. 4e), we reasoned that the transframe product produced by frameshifting at slippery site C had lower specific luciferase activity, and that frameshifting at slippery site B contributed to most of the detected luciferase activity as a consequence of +1 ribosome frameshifting. Taken together, these data suggest that N^1-methylpseudouridylation at defined mRNA sequences triggers ribosome +1 frameshifting; however, with appropriate mRNA sequence design, it is possible to ameliorate this issue.

Conclusions

We show that 1-methylΨ is a modified ribonucleotide that significantly increases +1 ribosomal frameshifting during mRNA translation and that cellular immunity to +1 frameshifted products can occur following vaccination with mRNA containing 1-methylΨ. To our knowledge, this is the first report that mRNA modification affects ribosomal frameshifting. Alongside this impact on host T cell immunity, the off-target effects of ribosomal frameshifting could include increased production of new B cell antigens. Other ribonucleotide modification strategies, such as incorporation of 5-methoxyU, significantly decreased translation efficiency of IVT mRNAs, which may limit clinical translation. Although we have shown that translation of N^1-methylpseudouridylated mRNA leads to +1 ribosomal frameshifting in vitro and in cultured cells, it is conceivable that other mistranslation events (such as leaky scanning) could also contribute to T cell responses to +1 frameshifted peptide antigens. We show that IVT mRNAs contain few nucleotide insertions and deletions, and this is not changed by 1-methylΨ incorporation. Our data show that +1 ribosomal frameshifting occurs at two characterized slippery sequences. Therefore, we believe that the minor band of approximately 50 kDa produced by Fluc+1FS mRNA translation is probably a consequence of several frameshifting events (Fig. 1e). Translation of mRNA containing 1-methylΨ leads to slower translation elongation, caused by altered aminoacyl-tRNA binding, which demonstrates why +1 ribosomal frameshifting does not occur during unmodified mRNA translation—both ribosome stalling and ribosome slippery sequences seem to be required for productive +1 ribosome frameshifting. Our mechanistic data are supported by previous observations of ribosomal frameshifting during translation of naturally occurring mRNAs, which implicate ribosome stalling and require ribosome slippery sequences for +1 frameshifting[21,26–28,33,34]. These findings are of particular importance to our fundamental understanding of how ribonucleotide modification affects mRNA translation, and for designing and optimizing future mRNA-based therapeutics to avoid mistranslation events that may decrease efficacy or increase toxicity.

Online content

Any methods, additional references, Nature Portfolio reporting summaries, source data, extended data, supplementary information, acknowledgements, peer review information; details of author contributions and competing interests; and statements of data and code availability are available at https://doi.org/10.1038/s41586-023-06800-3.

1. Hogan, M. J. & Pardi, N. mRNA vaccines in the COVID-19 pandemic and beyond. *Annu. Rev. Med.* **73**, 17–39 (2022).
2. Chaudhary, N., Weissman, D. & Whitehead, K. A. mRNA vaccines for infectious diseases: principles, delivery and clinical translation. *Nat. Rev. Drug Discov.* **20**, 817–838 (2021).
3. Anderson, B. R. et al. Incorporation of pseudouridine into mRNA enhances translation by diminishing PKR activation. *Nucleic Acids Res.* **38**, 5884–5892 (2010).
4. Holtkamp, S. et al. Modification of antigen-encoding RNA increases stability, translational efficacy, and T-cell stimulatory capacity of dendritic cells. *Blood* **108**, 4009–4017 (2006).
5. Andries, O. et al. N^1-methylpseudouridine-incorporated mRNA outperforms pseudouridine-incorporated mRNA by providing enhanced protein expression and reduced immunogenicity in mammalian cell lines and mice. *J. Control. Release* **217**, 337–344 (2015).
6. Boo, S. H. & Kim, Y. K. The emerging role of RNA modifications in the regulation of mRNA stability. *Exp. Mol. Med.* **52**, 400–408 (2020).
7. Squires, J. E. et al. Widespread occurrence of 5-methylcytosine in human coding and non-coding RNA. *Nucleic Acids Res.* **40**, 5023–5033 (2012).
8. Argoudelis, A. D. & Mizsak, S. A. 1-methylpseudouridine, a metabolite of *Streptomyces platensis*. *J. Antibiot.* **29**, 818–823 (1976).
9. Pang, H. et al. Structure of a modified nucleoside in archaebacterial tRNA which replaces ribosylthymine. 1-Methylpseudouridine. *J. Biol. Chem.* **257**, 3589–3592 (1982).
10. Brand, R. C., Klootwijk, J., Planta, R. J. & Maden, B. E. Biosynthesis of a hypermodified nucleotide in *Saccharomyces carlsbergensis* 17S and HeLa-cell 18S ribosomal ribonucleic acid. *Biochem. J.* **169**, 71–77 (1978).
11. Li, B., Luo, X. & Dong, Y. Effects of chemically modified messenger RNA on protein expression. *Bioconjugate Chem.* **27**, 849–853 (2016).
12. Zangi, L. et al. Modified mRNA directs the fate of heart progenitor cells and induces vascular regeneration after myocardial infarction. *Nat. Biotechnol.* **31**, 898–907 (2013).
13. Stadler, C. R. et al. Elimination of large tumors in mice by mRNA-encoded bispecific antibodies. *Nat. Med.* **23**, 815–817 (2017).
14. Pardi, N. et al. Nucleoside-modified mRNA immunization elicits influenza virus hemagglutinin stalk-specific antibodies. *Nat. Commun.* **9**, 3361 (2018).
15. Licht, K. et al. Inosine induces context-dependent recoding and translational stalling. *Nucleic Acids Res.* **47**, 3–14 (2019).
16. Hoernes, T. P. et al. Nucleotide modifications within bacterial messenger RNAs regulate their translation and are able to rewire the genetic code. *Nucleic Acids Res.* **44**, 852–862 (2016).
17. Karijolich, J. & Yu, Y. T. Converting nonsense codons into sense codons by targeted pseudouridylation. *Nature* **474**, 395–398 (2011).
18. Eyler, D. E. et al. Pseudouridinylation of mRNA coding sequences alters translation. *Proc. Natl Acad. Sci. USA* **116**, 23068–23074 (2019).
19. Kim, K. Q. et al. N1-methylpseudouridine found within COVID-19 mRNA vaccines produces faithful protein products. *Cell Rep.* **40**, 111300 (2022).
20. Svitkin, Y. V. et al. N1-methyl-pseudouridine in mRNA enhances translation through eIF2α-dependent and independent mechanisms by increasing ribosome density. *Nucleic Acids Res.* **45**, 6023–6036 (2017).
21. Bartok, O. et al. Anti-tumour immunity induces aberrant peptide presentation in melanoma. *Nature* **590**, 332–337 (2021).
22. Folegatti, P. M. et al. Safety and immunogenicity of the ChAdOx1 nCoV-19 vaccine against SARS-CoV-2: a preliminary report of a phase 1/2, single-blind, randomised controlled trial. *Lancet* **396**, 467–478 (2020).
23. Bhatt, P. R. et al. Structural basis of ribosomal frameshifting during translation of the SARS-CoV-2 RNA genome. *Science* **372**, 1306–1313 (2021).
24. Champagne, J., Mordente, K., Nagel, R. & Agami, R. Slippy-Sloppy translation: a tale of programmed and induced-ribosomal frameshifting. *Trends Genet.* **38**, 1123–1133 (2022).
25. Chen, T. H., Potapov, V., Dai, N., Ong, J. L. & Roy, B. N^1-methyl-pseudouridine is incorporated with higher fidelity than pseudouridine in synthetic RNAs. *Sci. Rep.* **12**, 13017 (2022).
26. Simms, C. L., Yan, L. L., Qiu, J. K. & Zaher, H. S. Ribosome collisions result in +1 frameshifting in the absence of no-go decay. *Cell Rep.* **28**, 1679–1689 (2019).
27. Juszkiewicz, S. & Hegde, R. S. Initiation of quality control during poly(A) translation requires site-specific ribosome ubiquitination. *Mol. Cell* **65**, 743–750 (2017).
28. O'Connor, M. Imbalance of tRNA(Pro) isoacceptors induces +1 frameshifting at near-cognate codons. *Nucleic Acids Res.* **30**, 759–765 (2002).
29. Stoneley, M. et al. Unresolved stalled ribosome complexes restrict cell-cycle progression after genotoxic stress. *Mol. Cell* **82**, 1557–1572 (2022).
30. Lareau, L. F., Hite, D. H., Hogan, G. J. & Brown, P. O. Distinct stages of the translation elongation cycle revealed by sequencing ribosome-protected mRNA fragments. *Elife* **3**, e01257 (2014).
31. Prokhorova, I. et al. Aminoglycoside interactions and impacts on the eukaryotic ribosome. *Proc. Natl Acad. Sci. USA* **114**, E10899–E10908 (2017).
32. Tuite, M. F. & McLaughlin, C. S. The effects of paromomycin on the fidelity of translation in a yeast cell-free system. *Biochim. Biophys. Acta* **783**, 166–170 (1984).
33. Jacks, T., Madhani, H. D., Masiarz, F. R. & Varmus, H. E. Signals for ribosomal frameshifting in the Rous sarcoma virus gag-pol region. *Cell* **55**, 447–458 (1988).
34. Devaraj, A. & Fredrick, K. Short spacing between the Shine-Dalgarno sequence and P codon destabilizes codon-anticodon pairing in the P site to promote +1 programmed frameshifting. *Mol. Microbiol.* **78**, 1500–1509 (2010).

Methods

Plasmids and mRNA synthesis

Phusion High-Fidelity DNA polymerase reagents were obtained from New England Biolabs. In-frame WT Fluc template DNA was produced by XbaI digest of pUCK100Fluc, including an 80-nucleotide polyA tail[29]. Fluc+1FS template DNA was produced by overlap extension PCR of pUCK100Fluc using FlucFlag_F (5′-TTATACCATGGGTGACTACAAAGACCATGACGGTGATTATAAAGATCATGACATCGATTACAAGGATGACGATGACAAGCTCGAAGACGCCAAAAACATAAAGAAAGG-3′), Fluc+1FS_R (5′-GATTGCCGAAAAATAGGATCTCTGGCATG-3′) for Fluc+1FS NFluc, Fluc+1FS_F (5′-CAGAGATCCTATTTTTCGGCAATCAAATCAT-3′) and Fluc_R (5′-TAGATTGCTAGCTTATGTTAATTACACGGCGATCTTTCCG-3′) for Fluc+1FS CFluc. PCR products were reinserted into pUCK100 using NcoI and NheI, and linear template DNA was produced by XbaI digest. A206G, U*187C and U*208C mRNA were transcribed from custom genes subcloned into pUC57T7 (Genscript Biotech) and linear template DNA was produced by BamHI digest. Fluc+1FS2 mRNA was produced from Fluc+1FS template DNA subcloned into pUC57T7 and linearized by BamHI. U*187C/U*208C template DNA was produced by overlap extension PCR and reinsertion into pUC57. Reporter RNA sequences are shown in Supplementary Fig. 1. In vitro transcription was carried out using TranscriptAid T7 High Yield Transcription Kit (Thermo Scientific K0441). UTP and CTP were substituted where required for 5-methoxyUTP, N^1-methylpseudoUTP or 5-methylCTP. Modified nucleotides were obtained from Trilink Biotechnologies. Transcripts were 5′-capped using the Vaccinia Capping System (NEB M2080S) and purified by phenol–chloroform extraction and G50 size exclusion. Transcripts were quantified using a Nanodrop ND2000 spectrophotometer (Thermo Scientific) and stored at −80 °C.

RNA gel electrophoresis

Samples were heated in formamide with bromophenol blue and xylene cyanol dye for 3 min at 95 °C, cooled for 2 min on ice and resolved on a 1% agarose formaldehyde MOPS acetate gel for 90 min at 90 V. The gel was stained in 0.5 μg ml^{-1} ethidium bromide for 1 h, bathed in distilled water for 1 h and visualized by UV transillumination.

Cell culture and mRNA transfection

HeLa cells were a gift from the Proudfoot Lab, University of Oxford. Cells were authenticated by STR typing. Cells were grown in DMEM (Gibco 41966029), supplemented with 10% FBS at 37 °C, 5% CO_2. Cells were tested for mycoplasma contamination and tested negative. Approximately 16 h before transfection, cells were seeded at 0.2×10^6 ml^{-1} in 6-well plates. Ten minutes before transfection, the medium was changed to OptiMEM (Gibco 31985062), after which cells were transfected with 4 pmol Fluc+1FS mRNA in Lipofectamine 2000 (Invitrogen 11668019). After 4 h transfection, OptiMEM was replaced with DMEM, and cells were cultured for a further 4 h, and then lysed in Passive Lysis Buffer (Promega E1941). Lysates were centrifuged (10,000*g*, 5 min) and luciferase activity was determined in supernatants using the Luciferase Assay System (Promega E4550) and GloMax multi-well plate luminometer (Promega).

In vitro translation

IVT mRNAs were translated using the Flexi Rabbit Reticulocyte Lysate System using nuclease-treated RRL (Promega L4540). For co-translational labelling, 0.33 μl translation-grade [^{35}S]methionine (Hartman Analytic KSM-01) and 0.67 μl amino acids minus methionine (Promega L996A) were used per 15 μl reaction. Unlabelled products were produced with 1 μl total (unlabelled) amino acids (Promega L4461). The concentration of IVT mRNA was 50 nM and, when included, the concentration of paromomycin (Sigma Aldrich P9297) was 100 μM. Creatine phosphate (Roche 10621714001), creatine kinase (Roche 21778721), potassium acetate (Sigma Aldrich P1190) and magnesium acetate (Sigma Aldrich M5661) were included at 10 mM, 25 μg ml^{-1}, 50 mM and 0.5 mM, respectively[35]. Reactions were incubated at 30 °C for the indicated time and moved to ice, after which 10 μl RNase A/T1 and Benzonase was added and incubated for 10 min. Luciferase activity was determined using the Luciferase Assay System (Promega E4550) and measured using a GloMax multi-well plate luminometer (Promega). The relative proportion of gain-of-function luciferase activity from Fluc+1FS mRNA translation was calculated by the relative light units (RLUs) for each mRNA translation reaction as a percentage of unmodified WT Fluc mRNA translation RLUs. For western blotting, 2× reducing LDS PAGE buffer was mixed with each sample, which was heated to 70 °C for 10 min. Cooled samples were resolved on NuPAGE 4–12% or 12%, Bis-Tris, 1.0 mm, Mini Protein Gels (Invitrogen). The resolved products were transferred to nitrocellulose membrane and probed using anti-Flag M2 antibody (Sigma Aldrich F1804) and anti-mouse-HRP antibody (Dako P0447), and detected with Clarity Western ECL substrate (Bio-Rad 1705060). Figures 1 and 4 show translation reactions from $n = 3$ replicates.

Peptide LC–MS/MS analysis

IVT mRNA was translated as above. After RNA digestion, translation products were immunoprecipitated using anti-Flag magnetic agarose beads (Pierce) overnight at 4 °C. Beads were washed twice in PBS, once in water, eluted in LDS PAGE buffer, and resolved on a NuPAGE 4–12%, Bis-Tris, 1.5 mm, Mini Protein Gel (NP0335BOX). The gel was stained with Coomassie dye and the region between about 60 kDa and 75 kDa (Precision Plus Protein All Blue Prestained Protein Standard; Bio-Rad) was excised and processed for mass spectrometry analysis as previously described[36]. In brief, the excised gel slice was cut into 1-mm pieces and placed in an 1.5-ml microtube. Coomassie staining was removed by incubating alternatively with a mixture of 25 mM ammonium bicarbonate and acetonitrile (2:1) and 25 mM ammonium bicarbonate. Each 15-min incubation at 37 °C was repeated until gel pieces were completely destained. Reduction and alkylation of cysteines was carried out by first incubating with a fresh 10 mM final concentration of dithiothreitol in 25 mM ammonium bicarbonate at 60 °C for 60 min and then changing the solution to 60 mM final concentration of iodoacetamide in 25 mM ammonium bicarbonate and incubating for an addition 45 min at room temperature in the dark. After dehydrating the gel pieces with acetonitrile, trypsin solution (10 ng μl^{-1} in 25 mM ammonium bicarbonate) or AspN (1 ng μl^{-1} in 25 mM ammonium bicarbonate) was added until gel pieces were completely covered. Digestion was carried at 37 °C for 16 h, 1,000 r.p.m. shaking. Proteases were inactivated by adding formic acid (trypsin digest) or TFA (AspN digest) to a final concentration of 1% (v/v). Peptides were extracted by sequential incubations with water/acetonitrile/formic acid (50:49:1 and 80:19:1% (v/v)). Extracted peptides were pooled and dried to completion and resuspended in water/acetonitrile (97:3% (v/v)) with 0.1% (v/v) TFA for mass spectrometry analysis. Mass spectrometry analysis was carried out once for trypsin digest and once for AspN digest.

Mass spectrometry analysis

In-gel digests were analysed using an Ultimate 3000 RSLC nano system (Thermo Scientific) coupled to an Orbitrap Eclipse mass spectrometer (Thermo Scientific). The sample was loaded onto the trapping column (Thermo Scientific, PepMap100, C18, 300 μm × 5 mm), using partial loop injection, for 3 min at a flow rate of 15 μl min^{-1} with 0.1% (v/v) FA in 3% acetonitrile. Peptides were separated on the analytical column (Easy-Spray C18 75 μm × 500 mm 2 μm column) at a flow rate of 300 nl min^{-1} using a gradient of 97% A (0.1% formic acid)/3% B (80% acetonitrile 0.1% formic acid) to 25% B over 50 min, then to 40% B for an additional 6 min, and then to 90% B for another 2 min, remaining at 90% B for 12 min before the percentage of B was then lowered to 3.8% to allow the column to re-equilibrate for 15 min before the next injection. Data were acquired using two field asymmetric ion mobility spectrometry CVs (−50 V, −70 V). For each field asymmetric ion mobility spectrometry experiment (maximum cycle time of 1.5 s per

experiment), data were acquired in data-dependent mode and MS1 consisted of a 120,000 resolution full-scan MS scan (AGC set to 100% (4×10^5 ions) with a maximum fill time of 50 ms) using a mass range of 380–1,500 m/z. The intensity MS2 trigger threshold was set to 5.0×10^3, and to avoid repeated selection of peptides for MS/MS, the experiment used a 40-s dynamic exclusion window. MS/MS was carried out on the Orbitrap using 30,000 resolution (AGC set to 100% (5×10^4 ions) with a maximum fill time of 54 ms). A higher-energy collisional dissociation collision energy of 32% was used to fragment the peptides and an isolation window of 1.2 was used.

Proteome Discoverer v2.5 analysis

Raw data were imported and data were processed in Proteome Discoverer (version 2.5, Thermo Fisher Scientific). The raw files were submitted to a database search using Proteome Discoverer with SequestHF against the *Oryctolagus cuniculus* (rabbit) database containing protein sequences from UniProt/Swiss-Prot (Proteome ID UP000001811), appended with Fluc (Uniprot ID P08659), predicted +1 frameshifted polypeptides and common contaminant proteins (several types of human keratin, BSA and porcine trypsin). The spectrum identification was carried out with the following parameters: MS accuracy, 10 ppm; MS/MS accuracy of 0.02 Da; up to two missed cleavage sites allowed; carbamidomethylation of cysteine; and oxidation of methionine as variable modifications. An interactive workflow was used in the processing step. After the first Sequest HT search, the Inferis Rescoring node was used and spectra with confidence worse than high were resubmitted for a second Sequest HT search using additional dynamic modifications (N and Q deamidation; N-terminal pyroglutamate; methionine loss and acetylation). Peptides were assigned to their respective reading frame or junction by inspection. Percolator node was used for false discovery rate estimation and only rank 1 peptide identifications of high confidence (false discovery rate < 1%) were accepted.

RNA-sequencing analysis

RNA-sequencing (RNA-seq) libraries were prepared from 1 µg IVT mRNA using NextFlex Rapid Directional RNA-seq kit 2.0 (PerkinElmer), according to the manufacturer's protocol. Libraries were amplified by six PCR cycles and purified by PAGE. Sequencing was carried out using an Illumina MiSeq at the Department of Biochemistry DNA sequencing facility, University of Cambridge (1 × 150 cycles V3). Reads were aligned with STAR (version 2.7.4a)[37]. Insertions and deletions per reference nucleotide were mapped from high-quality reads (QC score > 35) filtered for partial alignments and normalized to read depth. Insertion or deletion plots show the average mutation frequency for $n = 3$ replicated RNA-seq experiments.

SDS–PAGE autoradiography

IVT mRNAs were translated in nuclease-treated RRL (Promega) and products were co-translationally labelled as described above for 30 min. 2× LDS PAGE buffer was mixed to each sample, which was heated to 70 °C for 10 min. Cooled samples were resolved on NuPAGE 12%, Bis-Tris, 1.0 mm, Mini Protein Gels (Invitrogen NP0342BOX). The resolved gels were fixed in 10% methanol in acetic acid for 45 min, and dried at 80 °C for 2 h using a Fisher gel dryer system. Images were obtained by autoradiography using a Typhoon FLA 9000 and storage phosphor screens (GE Healthcare).

Incorporated [^{35}S]methionine quantification

IVT mRNAs were translated in nuclease-treated RRL (Promega) and products were co-translationally labelled for 2 h, as described above. [^{35}S]methionine incorporation was assayed according to the manufacturer's protocol. In brief, after RNA digestion, reactions were incubated for 10 min in 1 M NaOH. Polypeptides were precipitated in 5% TCA, collected on Whatman glass fibre filters, and washed three times with 5% TCA and once with acetone. The dried filters were immersed in 2 ml EcoScint liquid scintillation cocktail (National Diagnostics) and counted in a Tri-Carb 4910 TR liquid scintillation counter (PerkinElmer). Incorporated [^{35}S]methionine was determined from cpm of precipitated polypeptides per counts per minute of unwashed filters for each reaction (total counts per minute).

Mouse immunization

C57BL/6J mice (female, WT) were purchased from Charles Rivers Laboratories. Mice of 8–12 weeks old were intramuscularly injected with three doses of 10 µg BNT162b2, 5×10^7 infectious units of ChAdOx1 nCoV-19 or untreated. For booster immunizations, the same dose of the respective vaccine was injected 3 weeks and 6 weeks apart into the same site as the primary immunization. Spleens were obtained at day 8 post-third dose and cell suspensions were prepared. In brief, spleens were mashed with a syringe plunge and filtered through 70-µm cell strainers. Red blood cells were lysed with RBC lysing buffer (155 mM NH_4Cl, 12 mM $NaHCO_3$, 0.1 mM EDTA), before counting and cryopreserving before ELISpot assays. Mice were not randomly assigned to groups and experimenters were not blinded to experiments.

IFNγ ELISpot

Human IFNγ ELISpot assays were carried out as previously described using the human IFNγ ELISpot PLUS kit (ALP; MabTech 3420-4APT)[38]. Overlapping peptide pools corresponding to: in-frame SARS-CoV-2 spike protein (spike, 158 peptides); spike protein S1 and S2 regions (S1 + S2), which were described previously[38]; SARS-CoV-2 M protein, which was described previously[38]; and peptides predicted to occur by translation of the BNT162b2 mRNA +1 frame exclusively (+1FS spike, 123 peptides) were used. Peptides were obtained from Mimotopes, and are listed in Extended Data Table 3. Cryopreserved PBMCs were thawed in RPMI1640 medium supplemented with 1% (v/v) penicillin–streptomycin (Sigma), containing 0.01% (v/v) Benzonase nuclease (Merck). PBMCs were washed and then incubated for 1–2 h at 37 °C, 5% CO_2 in RPMI1640 medium, 10% (v/v) human AB serum and 1% (v/v) penicillin–streptomycin. Pre-coated IFNγ ELISpot 96-well plates (MabTech 3420-4APT-2) were washed three times with PBS and then blocked with RPMI1640 medium, 10% (v/v) human AB serum and 1% (v/v) penicillin–streptomycin for 45 min. Overlapping peptide pools were plated at 4 µg ml^{-1}, 50 µl per well; dimethylsulfoxide (Sigma) was used as the negative control at the equivalent concentration to the peptides. A total of 200,000 cells in 50 µl were added and incubated for 18–24 h. Cells were discarded, and plates were washed with PBS 0.05% (v/v) Tween (Sigma), and incubated with IFNγ detector antibody (clone 7-B6-1, 1 µg ml^{-1}) for 2–4 h at room temperature. Washed plates were then incubated with streptavidin alkaline phosphatase antibody (1 µg ml^{-1}) for 1–2 h. Plates were washed and then colour development was carried out using 1-step NBT/BCIP substrate solution. A 50 µl volume of filtered NBT/BCIP was added to each well for 5 min at room temperature after which development was stopped with cold water. Plates were dried at room temperature for approximately 48 h. Spots were quantified using an AID iSpot Spectrum EliSpot Reader (AID EliSpot Software version 7.0, Autoimmun Diagnostika). Average spot count value in the background wells was subtracted from that of the test wells and values were expressed as SFUs per million cells. Mouse IFNγ ELISpot assays were carried out using cryopreserved splenocytes thawed as above and incubated in RPMI1640 medium with 10% FBS alone. Peptide stimulations and downstream processing were as above, using pre-coated mouse IFNγ ELISpot PLUS kit (ALP; MabTech 3321-4APT-2). Figure 2b,c shows ELISpot responses for $n = 8$ mice per group. Figure 2d,e shows ELISpot responses for $n = 20$ ChAdOx1 nCoV-19-vaccinated individuals and $n = 21$ BNT162b2-vaccinated individuals.

HLA genotyping

HLA genotyping was conducted for $n = 40$ donors by Histogenetics LLC (Ossining, New York). HLA data (Extended Data Table 1) were filtered

to *HLA-A*, *HLA-B* and *HLA-C* genes and were truncated to allele group level. Donor genotypes for the BNT162b2-vaccinated individuals were visualized in a presence–absence heatmap in R (version 4.3.0) using ggplot2 (version 3.4.2). Major allele group information was summarized and individual allele group frequencies were calculated to illustrate the overall genetic composition.

Statistical analysis

Statistical analyses were carried out in base R (version 4.3.0) or using the DescTools R package (version 0.99.46).

Ethics statement

Animal experiments were licensed by the UK Home Office according to the Animals Scientific Procedures Act 1986 (License PP6047951), and approved and conducted in compliance with protocols by the University of Cambridge, University Biomedical Services Animal Welfare and Ethical Review Bodies committee. Human sample collection and analysis was conducted in accordance with the principles of good clinical practice and following approved protocols of the NIHR National BioResource. Samples were collected with the written informed consent of all study participants under the NIHR National BioResource-Research Tissue Bank ethics (research ethics committee (REC): 17/EE/0025) and from the PITCH study. PITCH is a substudy of the SIREN study, which was approved by the Berkshire REC, Health Research 250 Authority (IRAS ID 284460, REC reference 20/SC/0230), with PITCH recognized as a substudy on 2 December 2020. SIREN is registered with ISRCTN (Trial ID: 252 ISRCTN11041050). Some participants were recruited under aligned study protocols. In Liverpool, some participants were recruited under the study Human immune responses to acute virus infections (16/NW/0170), approved by North West - Liverpool Central REC on 8 March 2016, and amended on 14 September 2020 and 4 May 2021. In Oxford, participants were recruited under the GI Biobank Study 16/YH/0247, approved by the REC at Yorkshire & The Humber - Sheffield REC on 29 July 2016, which was amended for this purpose on 8 June 2020. The study was conducted in compliance with all relevant ethical regulations for work with human participants, and according to the principles of the Declaration of Helsinki (2008) and the International Conference on Harmonization Good Clinical Practice guidelines. Written informed consent to publish clinical and genetic data, as well as for study participation, was obtained for all participants enrolled in the study.

Reporting summary

Further information on research design is available in the Nature Portfolio Reporting Summary linked to this article.

Data availability

Mass spectrometry data have been deposited with MassIVE ID MSV000093074. RNA-seq reads and processed files are available at the NCBI Gene Expression Omnibus (accession GSE223044). Additional data are available from figshare (https://doi.org/10.6084/m9.figshare.24271744). The following accessions were used for mass spectrometry analysis: UP000001811 and P08659 (UniProt). Source data are provided with this paper.

Code availability

Scripts for processing alignments are available from GitHub[39].

35. Svitkin Y. V. & Sonenberg N. in *mRNA Processing and Metabolism* Vol. 257 (eds Schoenberg, D. R.) 155–170 (Humana, 2004).
36. Rosenfeld, J., Capdevielle, J., Guillemot, J. C. & Ferrara, P. In-gel digestion of proteins for internal sequence analysis after one- or two-dimensional gel electrophoresis. *Anal. Biochem.* **203**, 173–179 (1992).
37. Dobin, A. et al. STAR: ultrafast universal RNA-seq aligner. *Bioinformatics* **29**, 15–21 (2013).
38. Payne, R. P. et al. Immunogenicity of standard and extended dosing intervals of BNT162b2 mRNA vaccine. *Cell* **184**, 5699–5714 (2021).
39. Mulroney, T. E. RNA-seq_mutations. GitHub https://github.com/tom-mulroney/rna-seq_mutations (accessed 23 January 2023).

Acknowledgements A.E.W. and T.P. are supported by the Medical Research Council, grant number MC_UU_00025/7(A.E.W.). J.C.Y.-P., E.H., A.P.F. and J.E.D.T. are supported by the Medical Research Council (RG95376 and MC_UU_00025/12). T.E.M. was financially supported by the Integrative Toxicology Training Partnership. T.E.M., M.R., T.V.d.H., C.M.S., J.E.D.T., K.S.L. and A.E.W. acknowledge funding from Wellcome Leap as part of the R3 Program. PITCH was funded by the UK Department of Health and Social Care and UKRI (MR/W02067X/1 and MR/X009297/1), with contributions from UKRI/NIHR through the UK Coronavirus Immunology Consortium (UK-CIC), the Huo Family Foundation and The National Institute for Health Research (COV19-RECPLAS). In Liverpool PITCH is a sub-study of UKHSA's SIREN study. P.K. is an NIHR Senior Investigators and is funded by WT109965MA. S.J.D. is funded by an NIHR Global Research Professorship (NIHR300791). L.T. is supported by the Wellcome Trust (grant number 205228/Z/16/Z), the National Institute for Health Research Health Protection Research Unit (NIHR HPRU) in Emerging and Zoonotic Infections (EZI) (NIHR200907) and the Centre of Excellence in Infectious Diseases Research (CEIDR) and the Alder Hey Charity. This research was supported by the NIHR Cambridge Biomedical Research Centre (NIHR203312). The views expressed are those of the authors and not necessarily those of the NIHR or the Department of Health and Social Care. The authors thank the MRC Toxicology Unit Proteomics Facility for assistance with mass spectrometry analysis and A. Chong and D. Launer for assistance with DNA extraction and HLA typing.

Author contributions Conceptualization: T.E.M., J.E.D.T. and A.E.W.; methodology: T.E.M., T.P., M.S., E.H., A.J.M. and J.C.Y.-P.; investigation: T.E.M. (Figs. 1–4 and Extended Data Figs. 1–6), T.P. (Figs. 1 and 4), J.C.Y.-P. (Fig. 2b,c), M.R. (Fig. 2b,c), L.B. (Fig. 2e,f), A.P.F. (Fig. 2e,f), R.F.H. (Fig. 2b,c) and L.K. (Fig. 3, Extended Data Figs. 2 and 3 and Extended Data Table 2); writing (original draft): T.E.M., A.E.W. and J.E.D.T.; resources: L.T., P.K. and S.D.; data curation: T.E.M., J.E.D.T. and S.D.; writing (review and editing): T.E.M., A.E.W., J.E.D.T., T.P., M.S., P.K., S.D., C.M.S., T.V.d.H., K.S.L., A.J.M. and R.S.; visualization: T.E.M., L.K. and J.E.D.T.; supervision: A.E.W., J.E.D.T., T.P., T.E.M. and E.H.; project administration: J.E.D.T., A.E.W., C.M.S., T.V.d.H. and K.S.L.; funding acquisition: T.E.M., J.E.D.T., A.E.W., C.M.S., T.V.d.H. and K.S.L.

Competing interests T.E.M. and A.E.W. are inventors on a pending patent application (2305297.0) related to mRNA technology.

Additional information

Supplementary information The online version contains supplementary material available at https://doi.org/10.1038/s41586-023-06800-3.

Correspondence and requests for materials should be addressed to James E. D. Thaventhiran or Anne E. Willis.

Peer review information *Nature* thanks David Weiner and the other, anonymous, reviewer(s) for their contribution to the peer review of this work.

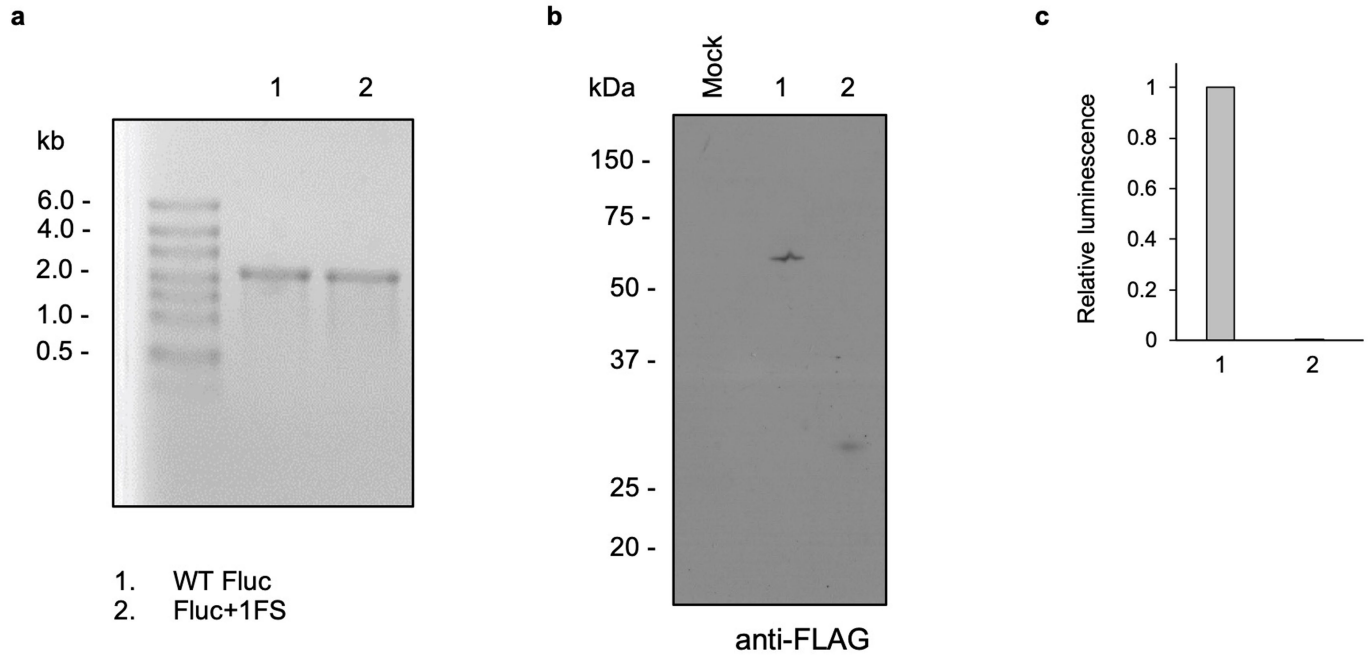

Extended Data Fig. 1 | Validation of WT Fluc, Fluc + 1FS, and Fluc-1FS mRNAs. a, UV photograph of WTFluc and Fluc+1FS mRNA transcripts analysed by agarose gel electrophoresis. **b**, Immunoblot of luciferase protein produced by translation of WTFluc and Fluc+1FS mRNAs using anti-FLAG antibody. **c**, Relative luciferase expression produced by translation of WTFluc and Fluc+1FS mRNAs. Data were obtained from $n = 1$ (non-replicated) analyses. For gel source data, see Supplementary Fig. 6.

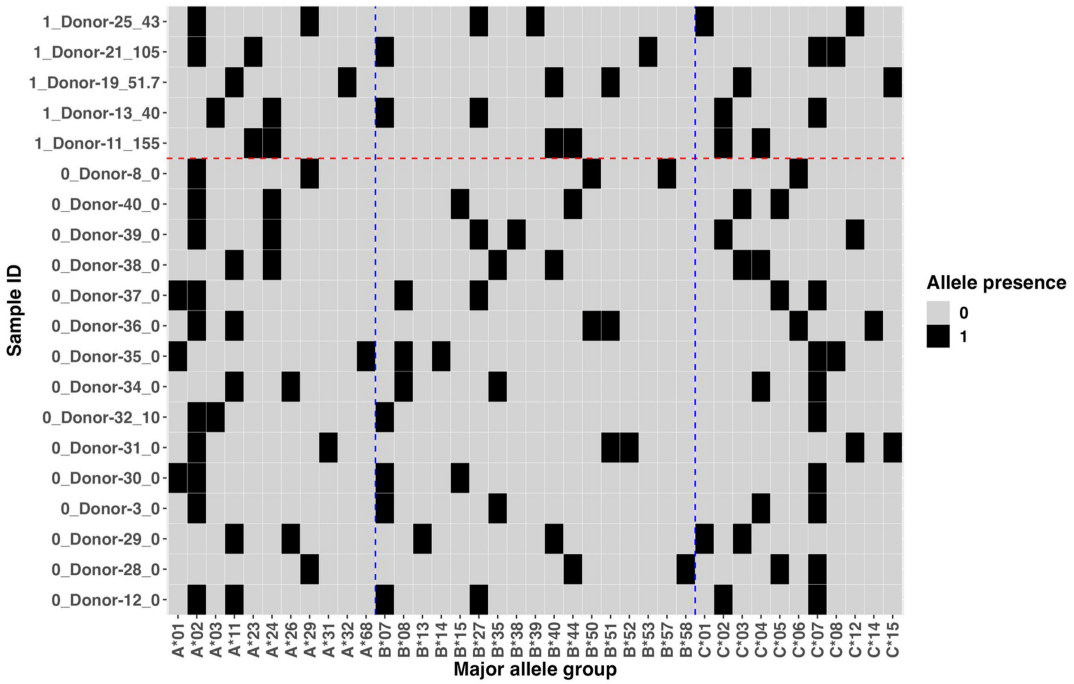

Extended Data Fig. 2 | Visualisation of HLA genotypes in BNT162b2-vaccinated individuals. Major allele groups in HLA-A, -B and -C genes for $n = 40$ donors. The Sample ID contains 3 fields separated by underline: (i) 1 or 0, with 1 denoting an ELISpot count >40 following stimulation with the +1 FS peptide pool; (ii) donor identifier; (iii) ELISpot count if >40. SFU/million. Allele group frequency indicated by black tile, vertical dashed lines: HLA genes, horizontal dashed line: indicates the cut-off (ELISpot count >40).

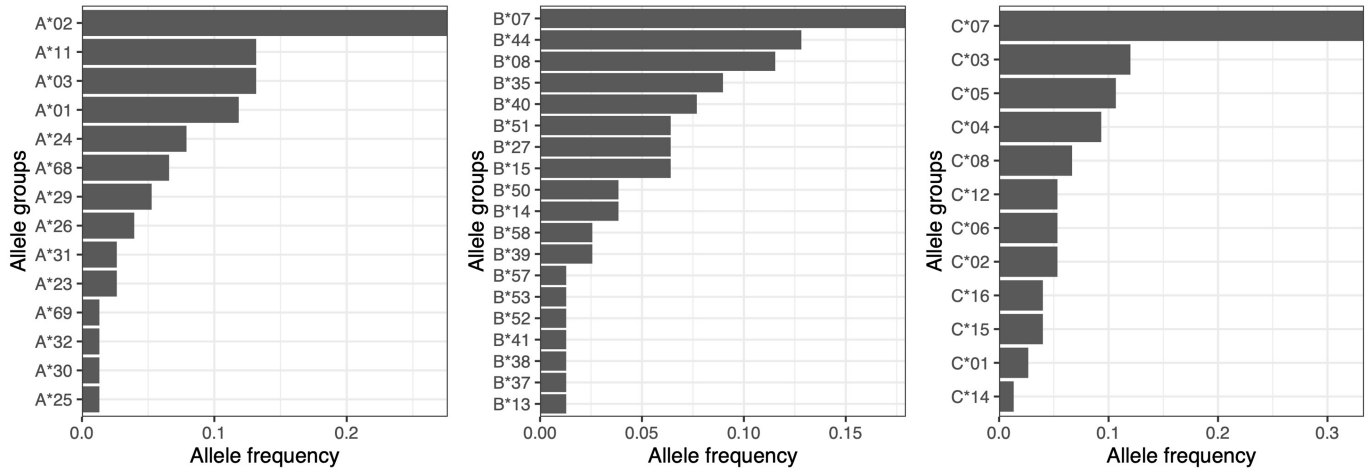

Extended Data Fig. 3 | HLA allele frequency distributions. Frequencies of each major allele group in HLA-A, -B and -C genes for $n = 40$ donors.

```
Query: SARS-CoV-2 S gene +1 frame translation
Sbjct: BNT162b2 mRNA +1 frame translation


Query  34    VFITLTKFSDPQFYIQLRTCSYLSFPMLLGSMLYMSLGPMVLRGLITLSYHLMMVFILLP  93
               T T+ SDP       RTCS LS     GS        PM  R   T          L
Sbjct  50    ACTTPTRCSDPACCTLPRTCSCLSS-ATPGSTPSTCPAPMAPRDSTTPCCPSTTGCTLPA  108

Query  94    LRSLT--EAGFLV--LLIRRPSPYLLLITLLMLLLKSVNFNFVMIHFWVFITTKTTKVGW  149
               RS T  EAG        R   P     T      K  + +       W   TT+TT+ GW
Sbjct  109   PRSPTSSEAGSSAPHWTAR---PRACSTTPPTWSSKCASSSSATTPSWASTTTRTTRAGW  165

Query  150   KVSSEFILVRIIALLNMSLSLFLWTLKENRVISKILGNLCLRILMVILKYILSTRLLI-C  208
               K SS        A  +   SL  WT K +R  S+   + CLR      +   ST L   C
Sbjct  166   KASSGCTAAPTTAPSSTCPSLS-WTWKASRATSRTCASSCLRTSTATSRSTASTPLSTSC  224

Query  209   VISLRVFRL--NHWIC-QVLTSLGFKLYLLYIEVILLVILLQVGQLVLQLIMWVIFNLGL  265
               I LR   L    WIC    TS GF+      E   L I    GQLV  L MW   +L
Sbjct  225   GICLRASLLWNPWWICPSASTSPGFRHCWPCTEATHLAIAAADGQLVPPLTMWATCSLEP  284

Query  266   FYNIMKMEPLQMLTVHLTLSQKQSVRNPS-LKKESIKLLTLESNQQNLLLDFLILQTCAL  324
               +  +  P     + L +  +QS  +PS  K+ S +  T   +  N      I   CA
Sbjct  285   SCSTTRTAPSPTPWIVLWILARQSAPSPSPWKRASTRPATSGCSPPNPSCGSPISPICAP  344

Query  325   LVKFLTPPDLHLFMLGTGRESATVLLIILSYIIPHHFPLLSVMECLLLNMISALLMSMQI  384
               +   PPD  L   GTG  SA           P      S   C L +   A
Sbjct  345   SARCSMPPDSPLCTPGTGSGSAIAWPTTPCCTTPPASAPSSATACPLPSTTCASQTCTPT  404

Query  385   HLLEVMKSDKSLQGKLERLLIIIIINYQMILQAALLGILTILILRLVVIIITCIDCLGSLI  444
                    MK  +    +  R      +      A L G  T    +     ITC  C GS I
Sbjct  405   ASSGEMKCGRLPLDRQARSPTTTTSCPTTSPAVLPGTATTWTPKSAATTITCTGCSGSPI  464

Query  445   SNLLREIFQLKSIRPVAHLVMVLKVLIVTFLYNHMVSNPLMVLVTNHTEYFLL-NFYMHQ  503
               S         +SIRP A LV   K    T   +    +P M    + TE++   N  M
Sbjct  465   SPSS-GTSPPRSIRPAAPLVTAWKASTATSHCSPTAFSPQMAWAISPTEWWCASNCCMPL  523

Query  504   QLFVDLKSLLIWLKTNVSISTSMVQAQVFLLSLTKSFCLSNNLAE-TLLTLLMLSVIHRH  562
                    L+   I  +TN   STS   A       T+S C S++LA  + +    L  I RH
Sbjct  524   PQCAALRKAPI-SRTNA-TSTSTAPAPACQR-ATRSSCHSSSLAGISPIPQTPL-EIPRH  579

Query  563   LRFLT--LHHVLLVVSVLHQEQILLTRLLFFIRMLTAQKSLLLFMQINLLLLGVFILQVL  620
               +  T  L      +S L     +  R     R  T  K    F  I+ L  G
Sbjct  580   WKSWTSPLAASAECLSPLAPTPAI--RWQCCTRT-TVPKCPWPFTPISHLHGGC-TPPAA  635

Query  621   MFFKHVQAVGLNMSTTHMSVTYPLVQVYALVIRLRLILLG-GHVVLVNPSLPTLCHLVQK  679
               M F+   AV    +T   S T P     A   R R   LG         SLPT C    +
Sbjct  636   MCFRPEPAVSEPSTTIATSATSPSALESAPATRHRQTALGEPEAWPARASLPTQCLWAPR  695

Query  680   IQLLTLITLLPYPQILLLVLPQKFYQCLPRHQ-IVQCTFVVIQLNAAIFCCNMAVFVHN-  737
                  T  TL    P       PQ+   C PR      CT   I  +A   CC+ A    +
Sbjct  696   TAWPTPTTLSLSPPTSPSA-PQRSCLCPPRPAWTAPCTSAAIPPSAPTCCCSTAASAPSI  754

Query  738   TVLLELLNKTKTPKKFLHKSNKFTKHHQLKILVVLIFHKYYQIHQNQARGHLLKIYFSTK  797
                      N+T+TPK+   KS + T+    +     I  ++  I  + A G   +   STK
Sbjct  755   EPQGSPWNRTRTPKRCSPKS-RSTRPLLSRTSAASISARFCPILASPASGASSRTCCSTK  813

Query  798   HLQMLASSNNMVIALVILLLETSFVHKSLTALLFCHLCSQMKLLNTLLHC-RVQSLLVGP  856
               H    ASS++M I    L     F  +SLT    C LC  M+  +T L C   QS   G
Sbjct  814   HWPTPASSSSMAIVWATLPPGI-FAPRSLTDQC-CLLC-PMRSPSTHLPCWPAQSQAAGH  870

Query  857   LVQVLHYKYHLLCKWLIGLMVLELHRMFSMRTKNLPTNLIVLLAKFKTHFLPQQVHLENF  916
               L Q    +  LLC+W  G    E  RM   RT++ PT+     A+ +T    QQ   E+
Sbjct  871   LEQAPLCRSPLLCRWPTGSTASEP-RMCCTRTRSSPTSSTAPSARSRTAAA-QQAPWESC  928

Query  917   KMWSTKMHKLTRLLNNLAPILVQFQVFMISFHVLTKLRLKCKLIGSQADFKVCRHMLNNL  976
               + WST+M + T   ++  P      +  IS    T LR +C+   SQAD +  RH  ++
Sbjct  929   RTWSTRMPRHTPWSSSCPPTSAPSALCTISAD-WTLLRPRCRSTDSQADCRASRHTPSSS  987

Query  977   ELQKSELLLILLLLKCQSVYLDNQKELIFVERAIILCPSLSQHLMVSS-CMLMSLHKKRT  1035
               E  + E L I    +C SV     +E  F  RA     SLS  L     C  M   K+R
Sbjct  988   EPPRLEPLPIWPPPRCLSVCWARAREWTFAARATTA--SLSLPLTAWCFCTHMCPLKRRI  1045

Query  1036  SQLLLPFVMMEKHTFLVKVSLFQMAHTGLHKGIFMNHKSLLQTTHLCLVTVMLELSTTQF  1095
               S  L P     K TFL K      A  G H G   + +S   TT  CL T      T
Sbjct  1046  SPPLQPSATTAKPTFLEKACSCPTAPIGSHSGTSTSPRSSPPTTPSCLATATSSALTIPC  1105

Query  1096  MILCNLN-THSRRS-INILRIIHHQMLIVTSLALMLQLTFKKKLTASMRLPRIMNLSSIS  1153
                 LC+ + T S+R+  + LR            A  +  +K +   R PRI   S+
Sbjct  1106  TTLCSPSWTASKRNWTSTLRTTQAPTWTWAISAESMPASTSRKRSTGTRWPRITRASTC-  1164

Query  1154  KNL  1156
               KN
Sbjct  1165  KNW  1167
```

Extended Data Fig. 4 | NCBI BLASTP alignment of +1 translated products. Protein BLAST alignment of polypeptides predicted by +1 frame translation of either BNT162b2 mRNA or Wuhan SARS-CoV-2 Spike mRNA (from NC_045512.2).

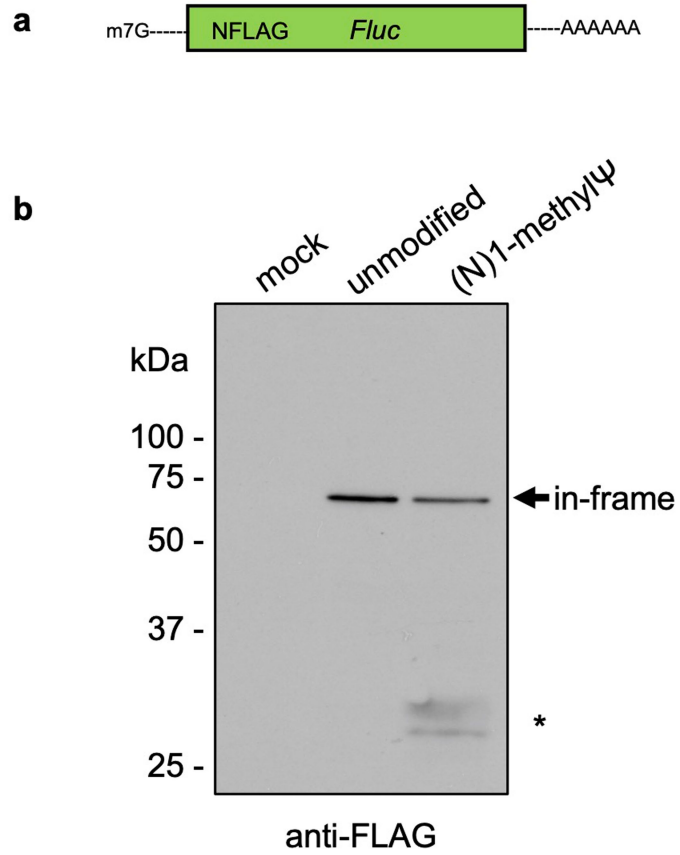

Extended Data Fig. 5 | Translation of 1-methylΨ-modified Fluc mRNA produces multiple polypeptides. a, Diagram of NFLAG-WTFluc mRNA. **b**, Western blot analysis (anti-FLAG epitope) of polypeptides produced by translation of unmodified, or 1-methylΨ, NFLAG-WTFluc mRNA. In-frame firefly luciferase is indicated by arrow. Low molecular weight polypeptides are indicated by asterisk (*). A single blot from $n = 3$ replicated experiments is displayed. For gel source data, see Supplementary Fig. 7.

>BNT162b2_Spike_mRNA_CDS

AmΨGmΨmΨCGmΨGmΨmΨCCmΨGGmΨGCmΨGCmΨGCCmΨCmΨGGmΨGmΨCCAGCCAGmΨGmΨGmΨGAACCmΨGACCACCAGAACACAGCmΨGCC
mΨCCAGCCmΨACACCAACAGCmΨmΨmΨACCAGAGGCGmΨGmΨACmΨACCCCGACAAGGmΨGmΨmΨCAGAmΨCCAGCGmΨGCmΨGCACmΨCmΨAC
CCAGGACCmΨGmΨmΨCCmΨGCCmΨmΨmΨCmΨmΨCAGCAACGmΨGACCmΨGGmΨmΨCCACGCCAmΨCCACGmΨGmΨCCGGCACCAAmΨGGCACC
AAGAGAmΨmΨCGACAACCCCGmΨGCmΨGCCCmΨmΨCAACGACGGGGmΨGmΨACmΨmΨmΨGCCAGCACCGAGAAGmΨCCAACAmΨCAmΨCAGAGGC
mΨGGAmΨCmΨmΨCGGCACCACACmΨGGACAGCAAGACCCAGAGCCmΨGCmΨGAmΨCGmΨGAACAACGCCACCAACGmΨGGmΨCAmΨCAAAGmΨGm
ΨGCGAGmΨmΨCCAGmΨmΨCmΨGCAACGACCCCmΨmΨCCmΨGGGCGmΨCmΨACmΨACCACAAGAACAACAAGAGCmΨGGAmΨGGAAAGCGAGmΨm
ΨCCGGGmΨGmΨACAGCAGCGCCAACAACmΨGCACCmΨmΨCGAGmΨACGmΨGmΨCCCAGCCmΨmΨmΨCCmΨGAmΨGGACCmΨGGAAGGCAAGCAG
GGCAACmΨmΨCAAGAACCmΨGCGCGAGmΨmΨCGmΨGmΨmΨmΨAAGAACAmΨCGACGGCmΨACmΨmΨCAAGAmΨCmΨACAGCAAGCACACCCCmΨ
AmΨCAACCmΨCGmΨGCGGGAmΨCmΨGCCmΨCAGGGCmΨmΨCmΨCmΨGCmΨCmΨGGAACCCCmΨGGmΨGGAmΨCmΨGCCCAmΨCGGCAmΨCAAC
AmΨCACCCGG*mΨmΨmΨC*AGACACmΨGCmΨGGCCCmΨGCACAGAAGCmΨACCmΨGACACCmΨGGCGAmΨAGCAGCAGCGGAmΨGGACAGCmΨGGmΨ
GCCGCCGCmΨmΨACmΨAmΨGmΨGGGCmΨACCmΨGCAGCCmΨAGAACCmΨmΨCCmΨGCmΨGAAGmΨACAACGAGAACGGCACCAmΨCACCGACGCC
GmΨGGAmΨmΨGmΨGCmΨCmΨGGAmΨCCmΨCmΨGAGCGAGACAAAGmΨGCACCCmΨGAAGmΨCCmΨmΨCACCGmΨGGAAAAGGGCAmΨCmΨACC
AGACCAGCAACmΨmΨCCGGGmΨGCAGCCCACCGAAmΨCCAmΨCGmΨGCGGmΨmΨCCCCAAmΨAmΨCACCAAmΨCmΨGmΨGCCCCmΨmΨCGGCGA
GGmΨGmΨmΨCAAmΨGCCACCAGAmΨmΨCGCCmΨCmΨGmΨGmΨACGCCmΨGGAACCGGAAGCGGAmΨCAGCAAmΨmΨGCGmΨGGCCGACmΨACm
ΨCCGmΨGCmΨGmΨACAACmΨCCGCCAGCmΨmΨCAGCACCmΨmΨCAAGmΨGCmΨACGGCGmΨGmΨCCCCmΨACCAAGCmΨGAACGACCmΨGmΨG
CmΨmΨCACAAACGmΨGmΨACGCCGACAGCmΨmΨCGmΨGAmΨCCGGGGAGAmΨGAAGmΨGCGGCAGAmΨmΨGCCCCmΨGGACAGACAGGCAAGAmΨ
CGCCGACmΨACAACmΨACAAGCmΨGCCCGACGACmΨmΨCACCGGCmΨGmΨGmΨGAmΨmΨGCCmΨGGAACAGCAACAACCmΨGGACmΨCCAAAGmΨ
CGGCGGCAACmΨACAAmΨmΨACCmΨGmΨACCGGCmΨGmΨmΨCCGGAAGmΨCCAAmΨCmΨGAAGCCCmΨmΨCGAGCGGGACAmΨCmΨCCACCGAG
AmΨCmΨAmΨCAGGCCGGCAGCACCCCmΨmΨGmΨAACGGCGmΨGGAAGGCmΨmΨCAACmΨGCmΨACmΨmΨCCCACmΨGCAGmΨCCmΨACGGC*mΨ*
*mΨmΨC*AGCCCACAAAmΨGGCGmΨGGGCmΨAmΨCAGCCCmΨACAGAGmΨGGmΨGGmΨGCmΨGAGCmΨmΨCGAACmΨGCmΨGCAmΨGCCCCmΨGC
CACAGmΨGmΨGCGGCCCmΨAAGAAAAGCACCAAmΨCmΨCGmΨGAAGAACAAAmΨGCGmΨGAACmΨmΨCAACmΨmΨCAACGGCCmΨGACCGGCACC
GGCGmΨGCmΨGACAGAGAGCAACAAGAAGmΨmΨCCmΨGCCAmΨmΨCCAGCAGmΨmΨmΨGGCCGGGAmΨAmΨCGCCGAmΨACCACAGACGCCGmΨm
ΨAGAGAmΨCCCCAGACACmΨGGAAAmΨCCmΨGGACAmΨCACCCCmΨmΨGCAGCmΨmΨCGGCGGAGmΨGmΨCmΨGmΨGAmΨCACCCCmΨGGCACC
AACACCAGCAAmΨCAGGmΨGGCAGmΨGCmΨGmΨACCAGGACGmΨGAACmΨGmΨACCGAAGmΨGCCCGmΨGGCCAmΨmΨCACGCCGAmΨCAGCmΨG
ACACCmΨACAmΨGGCGGGmΨGmΨACmΨCCACCGGCAGCAAmΨGmΨG*mΨmΨmΨC*AGACCAGAGCCGGCmΨGmΨCmΨGAmΨCGGAGCCGAGCACGm
ΨGAACAAmΨAGCmΨACGAGmΨGCGACAmΨCCCCAmΨCGGCGCmΨGGAAmΨCmΨGCGCCAGCmΨACCAGACACAGACAAACAGCCCmΨCGGAGAGCC
AGAAGCGmΨGGCCAGCCAGAGCAmΨCAmΨmΨGCCmΨACACAAmΨGmΨCmΨCmΨGGGCGCCGAGAACAGCGmΨGGCCmΨACmΨCCAACAACmΨCmΨ
AmΨCGCmΨAmΨCCCCACCAACmΨmΨCACCAmΨCAGCGmΨGACCACAGAGAmΨCCmΨGCCmΨGmΨGmΨCCAmΨGACCAAGACCAGCGmΨGGACmΨ
GCACCAmΨGmΨACAmΨCmΨGCGGCGAmΨmΨCCACCGAGmΨGCmΨCCAACCmΨGCmΨGCmΨGCAGmΨACGGCAGCmΨmΨCmΨGCACCCAGCmΨGA
AmΨAGAGCCCmΨGACAGGGAmΨCGCCGmΨGGAACAGGACAAGAACACCCAAGAGGmΨGmΨmΨCGCCCAAGmΨGAAGCAGAmΨCmΨACAAGACCCCm
ΨCCmΨAmΨCAAGGACmΨmΨCGGCGGCmΨmΨCAAmΨmΨmΨCAGCCAGAmΨmΨCmΨGCCCGAmΨCCmΨAGCAAGCCCAGCAAGCGGAGCmΨmΨCA
mΨCGAGGACCmΨGCmΨGmΨmΨCAACAAAGmΨGACACmΨGGCCGACGCCGGCmΨmΨCAmΨCAAGCAGmΨAmΨGGCGAmΨmΨGmΨCmΨGGGCGACA
mΨmΨGCCGCCAGGGAmΨCmΨGAmΨmΨmΨGCGCCCAGAAGmΨmΨmΨAACGGACmΨGACAGmΨGCmΨGCCmΨCCmΨCmΨGCmΨGACCGAmΨGAGA
mΨGAmΨCGCCCAGmΨACACAmΨCmΨGCCCmΨGCmΨGGCCGGCACAAmΨCACAAGCGGCmΨGGACAmΨmΨmΨGGAGCAGGCGCCGCmΨCmΨGCAGA
mΨCCCCmΨmΨmΨGCmΨAmΨGCAGAmΨGGCCmΨACCGGmΨmΨCAACGGCAmΨCGGAGmΨGACCCAGAAmΨGmΨGCmΨGmΨACGAGAACCAGAAGC
mΨGAmΨCGCCAACCAGmΨmΨCAACAGCGCCAmΨCGGCAAGAmΨCCAGGACAGCCmΨGAGCAGCACAGCAAGCGCCCmΨGGGAAAGCmΨGCAGGACGm
ΨGGmΨCAACCAGAAmΨGCCCAGGCACmΨGAACACCCmΨGGmΨCAAGCAGCmΨGmΨCCmΨCCAACmΨmΨCGGCGCCAmΨCAGCmΨCmΨGmΨGCmΨ
GAACGAmΨAmΨCCmΨGAGCAGACmΨGGACCCmΨCCmΨGAGGCCGAGGmΨGCAGAmΨCGACAGACmΨGAmΨCACAGGCAGACmΨGCAGAGCCmΨCC
AGACAmΨACGmΨGACCCAGCAGCmΨGAmΨCAGAGCCGCCGAGAmΨmΨAGAGCCmΨCmΨGCCAAmΨCmΨGGCCGCCACCAAGAmΨGmΨCmΨGAGmΨ
GmΨGmΨGCmΨGGGCCAGAGCAAGAGAGmΨGGAC*mΨmΨmΨmΨ*GCGGCAAGGGCmΨACCACCmΨGAmΨGAGCmΨmΨCCCmΨCAGmΨCmΨGCCCCm
ΨCACGGCGmΨGGmΨG*mΨmΨmΨC*mΨGCACGmΨGACAmΨAmΨGmΨGCCCGCmΨCAAGAGAAGAAmΨmΨmΨCACCACCGCmΨCCAGCCAmΨCmΨGC
CACGACGGCAAAGCCCAC*mΨmΨmΨC*CmΨAGAGAAGGCGmΨGmΨmΨCGmΨGmΨCCAACGGCACCCAmΨmΨGGmΨmΨCGmΨGACACAGCGGAACmΨ
mΨCmΨACGAGCCCCAGAmΨCAmΨCACCACCGACAACACCmΨmΨCGmΨGmΨCmΨGGCAACmΨGCGACGmΨCGmΨGAmΨCGGCAmΨmΨGmΨGAACA
AmΨACCGmΨGmΨACGACCCmΨCmΨGCAGCCCGAGCmΨGGACAGCmΨmΨCAAAGAGGAACmΨGGACAAGmΨACmΨmΨmΨAAGAACCACACAAGCCC
CGACGmΨGGACCmΨGGGCGAmΨAmΨCAGCGGAAmΨCAAmΨGCCAGCGmΨCGmΨGAACAmΨCCAGAAAGAGAmΨCGACCGGCmΨGAACGAGGmΨGG
CCAAGAAmΨCmΨGAACGAGAGCCmΨGAmΨCGACCmΨGCAAGAACmΨGGGGAAGmΨACGAGCAGmΨACAmΨCAAGmΨGGCCCmΨGGmΨACAmΨCmΨ
GGCmΨGGGCmΨmΨmΨAmΨCGCCGGACmΨGAmΨmΨGCCAmΨCGmΨGAmΨGGmΨCACAAmΨCAmΨGCmΨGmΨGmΨmΨGCAmΨGACCAGCmΨGCm
ΨGmΨAGCmΨGCCmΨGAAGGGCmΨGmΨmΨGmΨAGCmΨGmΨGGCAGCmΨGCmΨGCAAGmΨmΨCGACGAGGACGAmΨmΨCmΨGAGCCCGmΨGCmΨG
AAGGGCGmΨGAAACmΨGCACmΨACACAmΨGA

Ribosome slippery site

Extended Data Fig. 6 | Annotated BNT162b2 Spike mRNA CDS putative slippery sites. Putative ribosome slippery sites in BNT162b2 which were identified by the following formula: m1Ψm1Ψm1Ψ X, where m1Ψ is (N)1-methylpseudouridine and X is (N)1-methylpseudouridine or cytidine in the first nucleotide of the immediate downstream codon.

Extended Data Table 1 | LC-MS/MS analysis of Fluc + 1FS high-molecular weight polypeptide

Group ID	Checked	Confidence	Sequence	Modifications	Qvality PEP	Qvality q-value	Number of Proteins	Number of PSMs	Number of Missed Cleavages	Theo MHplus in Da	Confidence by Search Engine Sequest HT	Percolator q-Value by Search Engine Sequest HT	Percolator PEP by Search Engine Sequest HT	XCorr by Search Engine Sequest HT	Top Apex RT in min	Frame
9935	TRUE	High	GPAPFYPLEDGTAGEQLHK		0.000143	0.0008289	2	2	0	2026.98688	High	0.0007087	5.42E-05	2.02	39.85	in frame
33451	TRUE	High	YGLNTNHR		0.006271	0.0008289	2	2	0	974.48025	High	0.0007087	0.003422	1.54	17.78	in frame
6239	TRUE	High	ELLNSMGISQPTVVFVSK	1xOxidation [M6]	0.003792	0.0008289	2	1	0	1965.03614	High	0.0007087	0.001972	1.62	46.54	in frame
12509	TRUE	High	KLPIIQK		0.106022	0.0098011	3	2	1	839.5713	High	0.007388	0.07696	1.43	25.88	in frame
15467	TRUE	High	IIIMDSK	1xOxidation [M4]	0.052499	0.0036367	2	3	0	835.45937	High	0.002833	0.03515	1.72	23.99	in frame
29537	TRUE	High	TIALIMNSSGSTGLPK	1xOxidation [M6]	0.001001	0.0008289	2	1	0	1605.85163	High	0.0007087	0.000459	2.15	38.1	in frame
7693	TRUE	High	FEEELFLR		0.027871	0.0008289	2	2	0	1082.55169	High	0.0007087	0.01757	2.31	43.71	+1FS
33224	TRUE	High	YDLSNLHEIASGGAPLSK		9.19E-06	0.0008289	2	2	0	1871.94977	High	0.0007087	2.68E-06	2.98	41.34	+1FS
7351	TRUE	High	EVGEAVAK		0.017231	0.0008289	2	1	0	802.43051	High	0.0007087	0.01038	0.94	17.65	+1FS
23417	TRUE	High	QGYGLTETTSAILITPEGDDKPGAVGK		0.021509	0.0008289	2	1	0	2718.38323	High	0.0007087	0.01322	1.04	42.98	+1FS
32478	TRUE	High	VVPFFEAK		0.091782	0.0090845	2	1	0	936.51893	High	0.006893	0.06561	1.62	39.85	+1FS
29665	TRUE	High	TLGVNQR		0.020576	0.0008289	2	1	0	787.44208	High	0.0007087	0.01259	1.05	19.53	+1FS
9994	TRUE	High	GPMIMSGYVNNPEATNALIDK	2xOxidation [M3; M5]	4.34E-07	0.0008289	2	2	0	2267.06824	High	0.0007087	9.50E-08	3.74	39.39	+1FS
6401	TRUE	High	EIVDYVASQVTTAK		0.000109	0.0008289	2	2	0	1523.79516	High	0.0007087	4.02E-05	2.52	41.76	+1FS
9405	TRUE	High	GGVVFVDEVPK		0.003535	0.0008289	2	2	0	1145.6201	High	0.0007087	0.001817	2.87	38.97	+1FS

Tryptic peptides identified by purification and LC-MS/MS analysis of the high molecular weight product produced by 1-methylΨ Fluc+1FS mRNA translation.

Extended Data Table 2 | Insertion and Deletion Frequencies in unmodified and 1-methylΨ mRNAs

Sample group	Mean		S.D.	
	Deletions	Insertions	Deletions	Insertions
unmodified	0.000862	0.000832	0.000118	0.000079
1-methylΨ	0.000625	0.000848	0.000080	0.000263
P-value	0.05297	0.9311		

Comparison of single nucleotide deletion frequency or insertion frequency, normalised to total reads (%), for unmodified or 1-methylΨ mRNA (Welch's unpaired two-tailed T-test).

Article

Extended Data Table 3 | Spike and +1FS Spike peptides

Protein	Pool	Sequence
Spike	S1	MFVFLVLLPLVSSQCVNL
Spike	S1	PLVSSQCVNLTTRTQL
Spike	S1	CVNLTTRTQLPPAYTNSF
Spike	S1	QLPPAYTNSFTRGVYY
Spike	S1	TNSFTRGVYYPDKVFR
Spike	S1	GVYYPDKVFRSSVLHSTQ
Spike	S1	FRSSVLHSTQDLFLPFF
Spike	S1	STQDLFLPFFSNVTWF
Spike	S1	LPFFSNVTWFHAIHV
Spike	S1	NVTWFHAIHVSGTNGTKR
Spike	S1	HVSGTNGTKRFDNPVLPF
Spike	S1	KRFDNPVLPFNDGVYF
Spike	S1	VLPFNDGVYFASTEKSNI
Spike	S1	YFASTEKSNIIRGWIF
Spike	S1	KSNIIRGWIFGTTLDSK
Spike	S1	WIFGTTLDSKTQSLLIV
Spike	S1	DSKTQSLLIVNNATNVVI
Spike	S1	IVNNATNVVIKVCEFQF
Spike	S1	VVIKVCEFQFCNDPFLGV
Spike	S1	QFCNDPFLGVYYHKNNK
Spike	S1	LGVYYHKNNKSWMESEFR
Spike	S1	NKSWMESEFRVYSSANNC
Spike	S1	FRVYSSANNCTFEYV
Spike	S1	SANNCTFEYVSQPFLMDL
Spike	S1	YVSQPFLMDLEGKQGNFK
Spike	S1	DLEGKQGNFKNLREFVFK
Spike	S1	FKNLREFVFKNIDGYFKI
Spike	S1	FKNIDGYFKIYSKHTPI
Spike	S1	FKIYSKHTPINLVRDL
Spike	S1	HTPINLVRDLPQGFSAL
Spike	S1	RDLPQGFSALEPLVDLPI
Spike	S1	ALEPLVDLPIGINITRF
Spike	S1	LPIGINITRFQTLLALHR
Spike	S1	RFQTLLALHRSYLTPGDS
Spike	S1	HRSYLTPGDSSSGWTAGA
Spike	S1	DSSSGWTAGAAAYYVGYL
Spike	S1	GAAAYYVGYLQPRTFLLK
Spike	S1	YLQPRTFLLKYNENGTI
Spike	S1	LLKYNENGTITDAVDCAL
Spike	S1	TITDAVDCALDPLSETK
Spike	S1	CALDPLSETKCTLKSFTV
Spike	S1	TKCTLKSFTVEKGIY
Spike	S1	KSFTVEKGIYQTSNFRV
Spike	S1	GIYQTSNFRVQPTESIVR
Spike	S1	RVQPTESIVRFPNITNL
Spike	S1	IVRFPNITNLCPFGEVF
Spike	S1	TNLCPFGEVFNATRFASV
Spike	S1	VFNATRFASVYAWNRKRI
Spike	S1	SVYAWNRKRISNCVADY
Spike	S1	KRISNCVADYSVLYNSAS
Spike	S1	DYSVLYNSASFSTFKCY
Spike	S1	SASFSTFKCYGVSPTKL
Spike	S1	KCYGVSPTKLNDLCFTNV
Spike	S1	KLNDLCFTNVYADSFVIR
Spike	S1	NVYADSFVIRGDEVRQI
Spike	S1	VIRGDEVRQIAPGQTGKI
Spike	S1	QIAPGQTGKIADYNYKL
Spike	S1	GKIADYNYKLPDDFTGCV
Spike	S1	KLPDDFTGCVIAWNSNNL
Spike	S1	CVIAWNSNNLDSKVGGNY
Spike	S1	NLDSKVGGNYNYLYRLFR
Spike	S1	NYNYLYRLFRKSNLKPF
Spike	S1	LFRKSNLKPFERDISTEI
Spike	S1	PFERDISTEIYQAGSTPC
Spike	S1	EIYQAGSTPCNGVEGF
Spike	S1	STPCNGVEGFNCYFPL
Spike	S1	VEGFNCYFPLQSYGF
Spike	S1	CYFPLQSYGFQPTNGVGY
Spike	S1	GFQPTNGVGYQPYRVVVL
Spike	S1	GYQPYRVVVLSFELL
Spike	S1	RVVVLSFELLHAPATV
Spike	S1	FELLHAPATVCGPKK
Spike	S1	APATVCGPKKSTNLVKNK
Spike	S1	KKSTNLVKNKCVNFNF
Spike	S1	VKNKCVNFNFNGLTGTGV
Spike	S1	NFNGLTGTGVLTESNKKF
Spike	S1	GVLTESNKKFLPFQQFGR
Spike	S1	KFLPFQQFGRDIADTTDA
Spike	S1	GRDIADTTDAVRDPQTL
Spike	S1	TDAVRDPQTLEILDI
Spike	S1	DPQTLEILDITPCSFGGV
Spike	S1	DITPCSFGGVSVITPGTN
Spike	S1	GVSVITPGTNTSNQVAVL
Spike	S1	TNTSNQVAVLYQDVNCTE
Spike	S1	VLYQDVNCTEVPVAI
Spike	S1	VNCTEVPVAIHADQL
Spike	S1	VPVAIHADQLTPTWRVY
Spike	S1	DQLTPTWRVYSTGSNVF
Spike	S1	RVYSTGSNVFQTRAGCLI
Spike	S1	VFQTRAGCLIGAEHV
Spike	S1	AGCLIGAEHVNNSYECDI
Spike	S1	HVNNSYECDIPIGAGI
Spike	S1	ECDIPIGAGICASYQTQT
Spike	S2	GICASYQTQTNSPRRAR
Spike	S2	TQTNSPRRARSVASQSII
Spike	S2	ARSVASQSIIAYTMSL
Spike	S2	QSIIAYTMSLGAENSVAY
Spike	S2	SLGAENSVAYSNNSIAI
Spike	S2	VAYSNNSIAIPTNFTISV
Spike	S2	AIPTNFTISVTTEILPV
Spike	S2	ISVTTEILPVSMTKTSV
Spike	S2	LPVSMTKTSVDCTMYI
Spike	S2	KTSVDCTMYICGDSTECS
Spike	S2	YICGDSTECSNLLLQY
Spike	S2	TECSNLLLQYGSFCTQL
Spike	S2	LQYGSFCTQLNRALTGI
Spike	S2	TQLNRALTGIAVEQDK
Spike	S2	LTGIAVEQDKNTQEVF
Spike	S2	EQDKNTQEVFAQVKQIYK
Spike	S2	VFAQVKQIYKTPPIKDF
Spike	S2	IYKTPPIKDFGGFNFSQI
Spike	S2	DFGGFNFSQILPDPSK
Spike	S2	FSQILPDPSKPSKRSFI
Spike	S2	PSKPSKRSFIEDLLFNKV
Spike	S2	FIEDLLFNKVTLADAGFI
Spike	S2	KVTLADAGFIKQYGDCL
Spike	S2	GFIKQYGDCLGDIAARDL
Spike	S2	CLGDIAARDLICAQKF
Spike	S2	ARDLICAQKFNGLTVL
Spike	S2	AQKFNGLTVLPPLLTDEM
Spike	S2	VLPPLLTDEMIAQYTSAL
Spike	S2	EMIAQYTSALLAGTI
Spike	S2	YTSALLAGTITSGWTF
Spike	S2	AGTITSGWTFGAGAALQI
Spike	S2	ITFGAGAALQIPFAMQMAY
Spike	S2	QIPFAMQMAYRFNGIGV
Spike	S2	MAYRFNGIGVTQNVLY
Spike	S2	GIGVTQNVLYENQKLI
Spike	S2	NVLYENQKLIANQFNSAI
Spike	S2	LIANQFNSAIGKIQDSL
Spike	S2	SAIGKIQDSLSSTASAL
Spike	S2	DSLSSTASALGKLQDVV
Spike	S2	SALGKLQDVVNQNAQAL
Spike	S2	DVVNQNAQALNTLVKQL
Spike	S2	QALNTLVKQLSSNFGAI
Spike	S2	KQLSSNFGAISSVLNDIL
Spike	S2	AISSVLNDILSRLDKV
Spike	S2	NDILSRLDKVEAEVQIDR
Spike	S2	KVEAEVQIDRLITGRL
Spike	S2	QIDRLITGRLQSLQTVV
Spike	S2	GRLQSLQTVVTQQLIR
Spike	S2	QTVVTQQLIRAAEIR
Spike	S2	QQLIRAAEIRASANL
Spike	S2	AAEIRASANLAATKM
Spike	S2	ASANLAATKMSECVL
Spike	S2	AATKMSECVLGQSKRVDF
Spike	S2	VLGQSKRVDFCGKGYHLM
Spike	S2	DFCGKGYHLMSFPQSAPH
Spike	S2	LMSFPQSAPHGVVFLHV
Spike	S2	APHGVVFLHVTYVPAQEK
Spike	S2	HVTYVPAQEKNFTTAPAI
Spike	S2	EKNFTTAPAICHDGKAHF
Spike	S2	AICHDGKAHFPREGVFV
Spike	S2	AHFPREGVFVSNGTHWFV
Spike	S2	FVSNGTHWFVTQRNFY
Spike	S2	HWFVTQRNFYEPQII
Spike	S2	QRNFYEPQIITTDNTFV
Spike	S2	QIITTDNTFVSGNCDVVI
Spike	S2	FVSGNCDVVIGIVNNTVY
Spike	S2	VIGIVNNTVYDPLQPEL
Spike	S2	TVYDPLQPELDSFKEEL
Spike	S2	PELDSFKEELDKYFK
Spike	S2	FKEELDKYFKNHTSPDV
Spike	S2	YFKNHTSPDVDLGDISGI
Spike	S2	DVDLGDISGINASVVNI
Spike	S2	SGINASVVNIQKEIDRL
Spike	S2	VNIQKEIDRLNEVAKNL
Spike	S2	DRLNEVAKNLNESLIDL
Spike	S2	KNLNESLIDLQELGKY
Spike	S2	LIDLQELGKYEQYIKWPW
Spike	S2	KYEQYIKWPWYIWLGFI
Spike	S2	WPWYIWLGFIAGLIAIVM
Spike	S2	FIAGLIAIVMVTIMLCCM
Spike	S2	VMVTIMLCCMTSCCSCLK
Spike	S2	CMTSCCSCLKGCCSCGSC
Spike	S2	LKGCCSCGSCCKFDEDDS
Spike	S2	SCCKFDEDDSEPVLKGVK
Spike	S2	FDEDDSEPVLKGVKLHYT
Spike	Spike	MFVFLVLLPLVSSQCVNL
Spike	Spike	PLVSSQCVNLTTRTQL
Spike	Spike	NLTTRTQLPPAYTNSFTR
Spike	Spike	PPAYTNSFTRGVYYPDKV
Spike	Spike	TRGVYYPDKVFRSSVL
Spike	Spike	KVFRSSVLHSTQDLFLPF
Spike	Spike	HSTQDLFLPFFSNVTWF
Spike	Spike	LPFFSNVTWFHAIHV
Spike	Spike	FHAIHVSGTNGTKRF
Spike	Spike	TNGTKRFDNPVLPFNDGV
Spike	Spike	NPVLPFNDGVYFASTEK
Spike	Spike	GVYFASTEKSNIIRGWIF
Spike	Spike	KSNIIRGWIFGTTLDSK
Spike	Spike	KTQSLLIVNNATNVVIKV
Spike	Spike	NNATNVVIKVCEFQF
Spike	Spike	KVCEFQFCNDPFLGVYY
Spike	Spike	NDPFLGVYYHKNNKSWM
Spike	Spike	YHKNNKSWMESEFRVY
Spike	Spike	MESEFRVYSSANNCTFEY
Spike	Spike	SSANNCTFEYVSQPFLM
Spike	Spike	EYVSQPFLMDLEGKQGNF
Spike	Spike	MDLEGKQGNFKNLREFVF
Spike	Spike	NFKNLREFVFKNIDGYFK
Spike	Spike	VFKNIDGYFKIYSKHTPI
Spike	Spike	FKIYSKHTPINLVRDL
Spike	Spike	PINLVRDLPQGFSALEPL
Spike	Spike	PQGFSALEPLVDLPIGI
Spike	Spike	PLVDLPIGINITRFQTLL
Spike	Spike	INITRFQTLLALHRSYL
Spike	Spike	LLALHRSYLTPGDSSSGW
Spike	Spike	LTPGDSSSGWTAGAAAYY
Spike	Spike	GWTAGAAAYYVGYLQPR
Spike	Spike	RTFLLKYNENGTITDAV
Spike	Spike	ENGTITDAVDCALDPL
Spike	Spike	VDCALDPLSETKCTLKSF
Spike	Spike	SETKCTLKSFTVEKGIY
Spike	Spike	SFTVEKGIYQTSNFRV
Spike	Spike	YQTSNFRVQPTESIVRF
Spike	Spike	QPTESIVRFPNITNLCPF
Spike	Spike	FPNITNLCPFGEVFNATR
Spike	Spike	PFGEVFNATRFASVYAW
Spike	Spike	TRFASVYAWNRKRISNCV
Spike	Spike	CVADYSVLYNSASFSTFK
Spike	Spike	YNSASFSTFKCYGVSPTK
Spike	Spike	FKCYGVSPTKLNDLCF
Spike	Spike	TKLNDLCFTNVYADSFVI
Spike	Spike	TNVYADSFVIRGDEVRQI
Spike	Spike	VIRGDEVRQIAPGQTGKI
Spike	Spike	QIAPGQTGKIADYNYKL
Spike	Spike	KIADYNYKLPDDFTGCVI
Spike	Spike	LPDDFTGCVIAWNSNNL
Spike	Spike	VIAWNSNNLDSKVGGNY
Spike	Spike	LDSKVGGNYNYLYRLFRK
Spike	Spike	YNYLYRLFRKSNLKPFER
Spike	Spike	RKSNLKPFERDISTEIY
Spike	Spike	ERDISTEIYQAGSTPC
Spike	Spike	YQAGSTPCNGVEGFNCYF
Spike	Spike	NGVEGFNCYFPLQSYGF
Spike	Spike	YFPLQSYGFQPTNGVGY
Spike	Spike	FQPTNGVGYQPYRVVVL
Spike	Spike	GYQPYRVVVLSFELL
Spike	Spike	LSFELLHAPATVCGPKK
Spike	Spike	PATVCGPKKSTNLVKNK
Spike	Spike	KSTNLVKNKCVNFNFNGL
Spike	Spike	KCVNFNFNGLTGTGVL
Spike	Spike	TESNKKFLPFQQFGRDI
Spike	Spike	PFQQFGRDIADTTDAVR
Spike	Spike	IADTTDAVRDPQTLEIL
Spike	Spike	RDPQTLEILDITPCSF
Spike	Spike	ILDITPCSFGGVSVI
Spike	Spike	GGVSVITPGTNTSNQVAV
Spike	Spike	GTNTSNQVAVLYQDV
Spike	Spike	AVLYQDVNCTEVPVAI
Spike	Spike	CTEVPVAIHADQLTPTWR
Spike	Spike	HADQLTPTWRVYSTGSNV
Spike	Spike	WRVYSTGSNVFQTRAGCL
Spike	Spike	NVFQTRAGCLIGAEHV
Spike	Spike	CLIGAEHVNNSYECDIPI
Spike	Spike	NNSYECDIPIGAGICASY
Spike	Spike	PIGAGICASYQTQTNSPR
Spike	Spike	SYQTQTNSPRRARSV
Spike	Spike	PRRARSVASQSIIAYTM
Spike	Spike	SQSIIAYTMSLGAENSV
Spike	Spike	MSLGAENSVAYSNNSIAI
Spike	Spike	VAYSNNSIAIPTNFTISV
Spike	Spike	AIPTNFTISVTTEILPV
Spike	Spike	PVSMTKTSVDCTMYI
Spike	Spike	DCTMYICGDSTECSNLLL
Spike	Spike	DSTECSNLLLQYGSF
Spike	Spike	LLQYGSFCTQLNRALTGI
Spike	Spike	TQLNRALTGIAVEQDK
Spike	Spike	GIAVEQDKNTQEVFAQVK
Spike	Spike	NTQEVFAQVKQIYKTPPI
Spike	Spike	VKQIYKTPPIKDFGGFNF
Spike	Spike	PPIKDFGGFNFSQIL
Spike	Spike	NFSQILPDPSKPSKRSFI
Spike	Spike	PSKPSKRSFIEDLLFNKV
Spike	Spike	FIEDLLFNKVTLADAGFI
Spike	Spike	PFAMQMAYRFNGIGV
Spike	Spike	RFNGIGVTQNVLYENQKL
Spike	Spike	QNVLYENQKLIANQF
Spike	Spike	KLIANQFNSAIGKIQDSL
Spike	Spike	SAIGKIQDSLSSTASAL
Spike	Spike	SLSSTASALGKLQDVV
Spike	Spike	LGKLQDVVNQNAQALNTL
Spike	Spike	NQNAQALNTLVKQLSSNF
Spike	Spike	TLVKQLSSNFGAISSV
Spike	Spike	NFGAISSVLNDILSRL
Spike	Spike	LNDILSRLDPPEAEVQI
Spike	Spike	DPPEAEVQIDRLITGRL
Spike	Spike	IDRLITGRLQSLQTYV
Spike	Spike	LQSLQTYVTQQLIRAAEI
Spike	Spike	TQQLIRAAEIRASANL
Spike	Spike	EIRASANLAATKMSECVL
Spike	Spike	AATKMSECVLGQSKRVDF
Spike	Spike	VLGQSKRVDFCGKGYHLM
Spike	Spike	KRVDFCGKGYHLMSF
Spike	Spike	LMSFPQSAPHGVVFLHV
Spike	Spike	PHGVVFLHVTYVPAQEK
Spike	Spike	VTYVPAQEKNFTTAPAI
Spike	Spike	KNFTTAPAICHDGKAHF
Spike	Spike	ICHDGKAHFPREGVFV
Spike	Spike	FPREGVFVSNGTHWFV
Spike	Spike	SNGTHWFVTQRNFYEPQI
Spike	Spike	TQRNFYEPQIITTDNTFV
Spike	Spike	QIITTDNTFVSGNCDVVI
Spike	Spike	FVSGNCDVVIGIVNNTVY
Spike	Spike	VIGIVNNTVYDPLQPEL
Spike	Spike	VYDPLQPELDSFKEELDK
Spike	Spike	LDSFKEELDKYFKNHTSP
Spike	Spike	DKYFKNHTSPDVDLGDI
Spike	Spike	SPDVDLGDISGINASVV
Spike	Spike	ISGINASVVNIQKEIDRL
Spike	Spike	VNIQKEIDRLNEVAKNL
Spike	Spike	RLNEVAKNLNESLIDL
Spike	Spike	LNESLIDLQELGKYEQYI
Spike	Spike	QELGKYEQYIKWPWYIWL
Spike	Spike	YIKWPWYIWLGFIAGLI
Spike	Spike	WLGFIAGLIAIVMVTIML
Spike	Spike	GLIAIVMVTIMLCCM
Spike	Spike	TIMLCCMTSCCSCLK
Spike	Spike	CSCLKGCCSCGSCCKF
Spike	Spike	DEDDSEPVLKGVKLHY
Spike	Spike	SCGSCCKFDEDDSEPVLK
+1FS spike	+1FS spike	YSSGPHRLRENPP
+1FS spike	+1FS spike	CSCSWCCCLWCPASV
+1FS spike	+1FS spike	PPEHSCLQPTPTALPEAC
+1FS spike	+1FS spike	PTPTALPEACTTPTR
+1FS spike	+1FS spike	ACTTPTRCSDPACCTLPR
+1FS spike	+1FS spike	SDPACCTLPRTCSCL
+1FS spike	+1FS spike	PRTCSCLSSATPGSTPST
+1FS spike	+1FS spike	SATPGSTPSTCPAPMAPR
+1FS spike	+1FS spike	STCPAPMAPRDSTTPCCP
+1FS spike	+1FS spike	PRDSTTPCCPSTTGCTL
+1FS spike	+1FS spike	PCCPSTTGCTLPAPR
+1FS spike	+1FS spike	LPAPRSPTSSEAGSSAP
+1FS spike	+1FS spike	SSEAGSSAPHWTARPR
+1FS spike	+1FS spike	AGSSAPHWTARPRAC
+1FS spike	+1FS spike	TTPPTWSSKCASSSSATT
+1FS spike	+1FS spike	SSKCASSSSATTPSW
+1FS spike	+1FS spike	TTPSWASTTTRTTRAGWK
+1FS spike	+1FS spike	TTRTTRAGWKASSGCTAA
+1FS spike	+1FS spike	ASSGCTAAPTTAPSST
+1FS spike	+1FS spike	TAAPTTAPSSTCPSL
+1FS spike	+1FS spike	WTWKASRATSRTCASSCL
+1FS spike	+1FS spike	TSRTCASSCLRTSTATSR
+1FS spike	+1FS spike	CLRTSTATSRSTASTPL
+1FS spike	+1FS spike	SRSTASTPLSTSCGICLR
+1FS spike	+1FS spike	LSTSCGICLRASLLWNPW
+1FS spike	+1FS spike	GICLRASLLWNPWWI
+1FS spike	+1FS spike	PWWICPSASTSPGFRHCW
+1FS spike	+1FS spike	ICPSASTSPGFRHCW
+1FS spike	+1FS spike	HLAAAAPASQLVPPLTMW
+1FS spike	+1FS spike	GQLVPPLTMWATCSL
+1FS spike	+1FS spike	PPLTMWATCSLEPSC
+1FS spike	+1FS spike	STTRTAPSPTPWIVLWIL
+1FS spike	+1FS spike	SPSPWKRASTRPATSGC
+1FS spike	+1FS spike	STRPATSGCSPPNPSC
+1FS spike	+1FS spike	CSPPNPSCGSPSIPSI
+1FS spike	+1FS spike	GSPISPICAPSARCSM
+1FS spike	+1FS spike	CAPSARCSMPPDSPL
+1FS spike	+1FS spike	PPDSPLCTPGTGSGSAI
+1FS spike	+1FS spike	LCTPPGTGSGSAIAW
+1FS spike	+1FS spike	IAWPTTPCCTTPPASAP
+1FS spike	+1FS spike	CTTPPASAPSSATACPL
+1FS spike	+1FS spike	TTCASQTCTPTA
+1FS spike	+1FS spike	SGEMKCGRLPLDRQAR
+1FS spike	+1FS spike	LPLDRQARSPTTTTSCPT
+1FS spike	+1FS spike	SPTTTTSCPTTSPAV
+1FS spike	+1FS spike	LPGTATTWTPKSAATTI
+1FS spike	+1FS spike	TPKSAATTITCTGCSGSP
+1FS spike	+1FS spike	AATTITCTGCSGSPI
+1FS spike	+1FS spike	SPSSGTSPPRSIRPAAPL
+1FS spike	+1FS spike	PRSIRPAAPLVTAWK
+1FS spike	+1FS spike	STATSHCSPTAFSPQMAW
+1FS spike	+1FS spike	PTAFSPQMAWAISPTEWW
+1FS spike	+1FS spike	ASNCCMPLPQCAALRK
+1FS spike	+1FS spike	CMPLPQCAALRKAPI
+1FS spike	+1FS spike	QRATRSSCHSSSLAGI
+1FS spike	+1FS spike	HSSSLAGISPIPQTPLEI
+1FS spike	+1FS spike	SPIPQTPLEIPRHWKSW
+1FS spike	+1FS spike	PLEIPRHWKSWTSPL
+1FS spike	+1FS spike	WKSWTSPLAASAECL
+1FS spike	+1FS spike	SPLAPTPAIRWQCCTR
+1FS spike	+1FS spike	TVPKCPWPFTPI
+1FS spike	+1FS spike	HLHGGCTPPAAMCFR
+1FS spike	+1FS spike	CTPPAAMCFRPEPAV
+1FS spike	+1FS spike	TIATSATPSALESAPAT
+1FS spike	+1FS spike	PSALESAPATRHRQTAL
+1FS spike	+1FS spike	ATRHRQTALGEPEAWPAR
+1FS spike	+1FS spike	LGEPEAWPARASLPTQCL
+1FS spike	+1FS spike	ARASLPTQCLWAPRTAW
+1FS spike	+1FS spike	CLWAPRTAWPTPTTLSL
+1FS spike	+1FS spike	WPTPTTLSLSPPTSPSA
+1FS spike	+1FS spike	PQRSCLCP
+1FS spike	+1FS spike	PRPAWTAPCTSAAIPPSA
+1FS spike	+1FS spike	CTSAAIPPSAPTCCCSTA
+1FS spike	+1FS spike	PSAPTCCCSTAASAP
+1FS spike	+1FS spike	QGSPWNRTRTPKRCSPK
+1FS spike	+1FS spike	SRSTRPLLSRTSAASI
+1FS spike	+1FS spike	SRTSAASISARFCPIL
+1FS spike	+1FS spike	SARFCPILASPASGASSR
+1FS spike	+1FS spike	ASPASGASSRTCCSTK
+1FS spike	+1FS spike	HWPTPASSSSMAIVWATL
+1FS spike	+1FS spike	SSSMAIVWATLPPGI
+1FS spike	+1FS spike	SPSTHLPCWPAQSQAA
+1FS spike	+1FS spike	WPAQSQAAGHLEQAPLCR
+1FS spike	+1FS spike	GHLEQAPLCRSPLLCRW
+1FS spike	+1FS spike	CRSPLLCRWPTGSTA
+1FS spike	+1FS spike	PRMCCTRTR
+1FS spike	+1FS spike	SPTSSTAPSARSR
+1FS spike	+1FS spike	AAQQAPWESCRTWSTRM
+1FS spike	+1FS spike	APWESCRTWSTRMPR
+1FS spike	+1FS spike	TPWSSSCPPTSAPSAL
+1FS spike	+1FS spike	ADWTLLRPRCRST
+1FS spike	+1FS spike	SQADCRASRHT
+1FS spike	+1FS spike	SEPPRLEPLPIWPPPRCL
+1FS spike	+1FS spike	LPIWPPPRCLSVCWARAR
+1FS spike	+1FS spike	CLSVCWARAREWTFAAR
+1FS spike	+1FS spike	WARAREWTFAARATT
+1FS spike	+1FS spike	ASLSLPLTAWCFCT
+1FS spike	+1FS spike	HMCPLKRRISPPLQPSAT
+1FS spike	+1FS spike	ISPPLQPSATTAKPTFL
+1FS spike	+1FS spike	LQPSATTAKPTFLEK
+1FS spike	+1FS spike	PTFLEKACSCPTAPI
+1FS spike	+1FS spike	HSGTSTSPRSSPPTTPSC
+1FS spike	+1FS spike	RSSPPTTPSCLATAT
+1FS spike	+1FS spike	TIPCTTLCSPSWTASKR
+1FS spike	+1FS spike	SPSWTASKRNWTSTLR
+1FS spike	+1FS spike	RNWTSTLRTTQAPTWTW
+1FS spike	+1FS spike	TTQAPTWTWAISAESM
+1FS spike	+1FS spike	APTWTWAISAESMPA
+1FS spike	+1FS spike	STCKNWGSTSSTSSGPGT
+1FS spike	+1FS spike	TSSTSSGPGTSGWAL
+1FS spike	+1FS spike	STSSGPGTSGWALSP
+1FS spike	+1FS spike	WSQSCCVA
+1FS spike	+1FS spike	RAVVAVAAAASSTRTIL
+1FS spike	+1FS spike	VAAAASSTRTILSPC
+1FS spike	+1FS spike	SSWYCMHAMLAAPFPSWV
+1FS spike	+1FS spike	MLAAPFPSWVPRVSPDL
+1FS spike	+1FS spike	WVPRVSPDLGSQVCSHL
+1FS spike	+1FS spike	LGSQVCSHLHLPHSPPLL
+1FS spike	+1FS spike	LHLPHSPPLLVPDTSQAR
+1FS spike	+1FS spike	LLVPDTSQARSNAAQNA
+1FS spike	+1FS spike	PLAINESLTKLY
+1FS spike	+1FS spike	PQGWSISCQPHPGA

List of peptides in each pool used for Spike and +1FS Spike ELISpot analysis.

nature portfolio

Corresponding author(s): Anne Willis, James Thaventhiran

Last updated by author(s): 13/10/23

Reporting Summary

Nature Portfolio wishes to improve the reproducibility of the work that we publish. This form provides structure for consistency and transparency in reporting. For further information on Nature Portfolio policies, see our Editorial Policies and the Editorial Policy Checklist.

Statistics

For all statistical analyses, confirm that the following items are present in the figure legend, table legend, main text, or Methods section.

n/a	Confirmed	
☐	☒	The exact sample size (*n*) for each experimental group/condition, given as a discrete number and unit of measurement
☐	☒	A statement on whether measurements were taken from distinct samples or whether the same sample was measured repeatedly
☐	☒	The statistical test(s) used AND whether they are one- or two-sided *Only common tests should be described solely by name; describe more complex techniques in the Methods section.*
☒	☐	A description of all covariates tested
☐	☒	A description of any assumptions or corrections, such as tests of normality and adjustment for multiple comparisons
☐	☒	A full description of the statistical parameters including central tendency (e.g. means) or other basic estimates (e.g. regression coefficient) AND variation (e.g. standard deviation) or associated estimates of uncertainty (e.g. confidence intervals)
☐	☒	For null hypothesis testing, the test statistic (e.g. *F*, *t*, *r*) with confidence intervals, effect sizes, degrees of freedom and *P* value noted *Give P values as exact values whenever suitable.*
☒	☐	For Bayesian analysis, information on the choice of priors and Markov chain Monte Carlo settings
☒	☐	For hierarchical and complex designs, identification of the appropriate level for tests and full reporting of outcomes
☒	☐	Estimates of effect sizes (e.g. Cohen's *d*, Pearson's *r*), indicating how they were calculated

Our web collection on statistics for biologists contains articles on many of the points above.

Software and code

Policy information about availability of computer code

Data collection	AID EliSpot Software (version 7.0), Proteome Discoverer (version 2.5).
Data analysis	R (version 4.3.0), ggplot2 (version 3.4.2), DescTools (version 0.99.46), STAR (version 2.7.4a). Scripts for analysis of RNA-seq data are available at: https://github.com/tom-mulroney/rna-seq_mutations.

For manuscripts utilizing custom algorithms or software that are central to the research but not yet described in published literature, software must be made available to editors and reviewers. We strongly encourage code deposition in a community repository (e.g. GitHub). See the Nature Portfolio guidelines for submitting code & software for further information.

Data

Policy information about availability of data

All manuscripts must include a data availability statement. This statement should provide the following information, where applicable:

- Accession codes, unique identifiers, or web links for publicly available datasets
- A description of any restrictions on data availability
- For clinical datasets or third party data, please ensure that the statement adheres to our policy

Mass spectrometry data have been deposited with MassIVE ID MSV000093074. RNA-seq reads and processed files are available at NCBI Gene Expression Omnibus (Accession GSE223044). Additional data are available from Figshare (DOI: 10.6084/m9.figshare.24271744). The following accessions were used for mass spectrometry analysis: UP000001811 and P08659 (UniProt).

Human research participants

Policy information about studies involving human research participants and Sex and Gender in Research.

Reporting on sex and gender	Sex and gender were not considered during study design. 37% of study participants were male. 63% were female. These data are included in Supplementary Table 1.
Population characteristics	Age, sex.
Recruitment	Participants were initially recruited as part of observational studies of the COVID-19 vaccine responses (https://doi.org/10.1016/j.cell.2021.10.011, https://doi.org/10.1038/s41591-023-02343-2, https://doi.org/10.1038/s41467-023-38810-0). Excess available samples from healthy vaccinated participants were subject to analysis. There are no recruitment biases identified that are likely to impact results.
Ethics oversight	Human sample collection and analysis was conducted in accordance with the principles of Good Clinical Practice and following approved protocols of the NIHR National Bioresource. Samples were collected with the written informed consent of all study participants under the NIHR National BioResource-Research Tissue Bank (NBR-RTB) ethics (REC:17/EE/0025) and from the PITCH study. PITCH is a sub-study of the SIREN study, which was approved by the Berkshire Research Ethics Committee, Health Research 250 Authority (IRAS ID 284460, REC reference 20/SC/0230), with PITCH recognised as a sub-study on 2nd December 2020. SIREN is registered with ISRCTN (Trial ID:252 ISRCTN11041050). Some participants were recruited under aligned study protocols. In Liverpool, some participants were recruited under the "Human immune responses to acute virus infections" Study (16/NW/0170), approved by North West - Liverpool Central Research Ethics Committee on 8th March 2016, and amended on 14th September 2020 and 4th May 2021. In Oxford, participants were recruited under the GI Biobank Study 16/YH/0247, approved by the research ethics committee (REC) at Yorkshire & The Humber - Sheffield Research Ethics Committee on 29th July 2016, which has been amended for this purpose on 8th June 2020. The study was conducted in compliance with all relevant ethical regulations for work with human participants, and according to the principles of the Declaration of Helsinki (2008) and the International Conference on Harmonization (ICH) Good Clinical Practice (GCP) guidelines. Written informed consent to publish clinical and genetic data, in addition to study participation was obtained for all participants enrolled in the study.

Note that full information on the approval of the study protocol must also be provided in the manuscript.

Field-specific reporting

Please select the one below that is the best fit for your research. If you are not sure, read the appropriate sections before making your selection.

☒ Life sciences ☐ Behavioural & social sciences ☐ Ecological, evolutionary & environmental sciences

For a reference copy of the document with all sections, see nature.com/documents/nr-reporting-summary-flat.pdf

Life sciences study design

All studies must disclose on these points even when the disclosure is negative.

Sample size	Sample sizes for mouse experiments were determined based on previous analysis. Because antigen-specific CD8+ T cell numbers are likely to be a continuous trait, the widely-accepted formula for calculating sample sizes for continuous variable published by Snedecor and Cochran (1989) has been used (https://doi.org/10.1017/S0021859600074104), with the following variable (s = standard deviation (~10% of mean - per previous mouse experiments in the lab), d = desired effect size to detect (± 15% of mean), C = constant dependent on the value of α and β (in this case 7.85; see https://doi.org/10.1093/ilar.43.4.207, α = 0.05, β = 0.2 (so that power = 80% i.e. 1 - β)). So: n = 1 + ((2 x 7.85) x (0.1/0.15)2) = 7.97 (i.e. 8 in each sample group). Human sample sizes were limited due to available excess PBMC samples from recruited study participants of studies of the COVID-19 vaccine response (https://doi.org/10.1016/j.cell.2021.10.011, https://doi.org/10.1038/s41591-023-02343-2, https://doi.org/10.1038/s41467-023-38810-0). A power analysis calculation for available samples was performed using MESS R package (version 0.5.9) prior to analysis based on effect sizes from previous experiments for n=20, n=21 (2-groups, one-tail, unequal variance, p=0.05), yielding power>0.8. Sample sizes for in vitro experiments were determined by previous similar experiments (e.g. https://doi.org/10.1093/nar/gkq347).
Data exclusions	No data were excluded from analysis.
Replication	All attempts at replication are included in the figures.
Randomization	Randomisation was not applicable at this was a non-interventional study.
Blinding	Blinding was not applicable at this was a non-interventional study.

Reporting for specific materials, systems and methods

We require information from authors about some types of materials, experimental systems and methods used in many studies. Here, indicate whether each material, system or method listed is relevant to your study. If you are not sure if a list item applies to your research, read the appropriate section before selecting a response.

Materials & experimental systems

n/a	Involved in the study
☐	☒ Antibodies
☐	☒ Eukaryotic cell lines
☒	☐ Palaeontology and archaeology
☐	☒ Animals and other organisms
☒	☐ Clinical data
☒	☐ Dual use research of concern

Methods

n/a	Involved in the study
☒	☐ ChIP-seq
☒	☐ Flow cytometry
☒	☐ MRI-based neuroimaging

Antibodies

Antibodies used: anti-FLAG M2 (Primary antibody raised in mouse)(Sigma Aldrich F1804), anti-mouse-HRP (secondary antibody raised in goat)(Dako P0447), anti-FLAG magnetic agarose (primary antibody conjugate raised in rat, Thermo Scientific A36797), IFNγ detector antibody clone 7-B6-1 (included in MabTech 3420-4APT kit).

Validation: anti-FLAG M2 antibody (Sigma Aldrich F1804) has been extensively validated by previous studies and the manufacturer for western blotting (e.g. https://doi.org/10.1186/s12985-016-0610-7, https://doi.org/10.1016/j.bbamcr.2019.06.002.). anti-FLAG magnetic agarose (Thermo Scientific A36797) has been validated for immunoprecipitation (e.g. https://doi.org/10.1002/cpz1.156). IFNγ detector antibody clone 7-B6-1 has been validated for ELISpot (e.g. https://doi.org/10.1016/j.cell.2020.08.017.).

Eukaryotic cell lines

Policy information about cell lines and Sex and Gender in Research

Cell line source(s)	HeLa cells (sex female) were obtained from ATCC.
Authentication	HeLa cells were independently authenticated by STR typing.
Mycoplasma contamination	HeLa cells were tested for mycoplasma infection and tested negative for mycoplasma infection.
Commonly misidentified lines (See ICLAC register)	HeLa cells are not a Misidentified Cell Line according to ICLAC register Version 12 (2023).

Animals and other research organisms

Policy information about studies involving animals; ARRIVE guidelines recommended for reporting animal research, and Sex and Gender in Research

Laboratory animals	C57BL/6J mice (wild type, WT) were purchased from Charles River laboratories. Mice were used at 8-12 weeks age. Mice were housed at the University of Cambridge as specific pathogen-free/SPF, 19-23 degrees Celsius, and the humidity is kept 45%-65%, a 12 hour (7am- 7pm) light dark cycle.
Wild animals	No wild animals were used in the study.
Reporting on sex	Sex was not considered in the study design. All mice were female.
Field-collected samples	No field collected samples were used in the study.
Ethics oversight	Animal experiments were licensed by the UK Home Office according to the Animals Scientific Procedures Act 1986 (License PP6047951), approved and conducted in compliance with protocols by the University of Cambridge, University Biomedical Services Animal Welfare and Ethical Review Bodies (AWERB) committee.

Note that full information on the approval of the study protocol must also be provided in the manuscript.